Geological Survey of Canada

CURRENT RESEARCH
2006-F1

U-Pb geochronology of the Neoarchean Swayze sector of the southern Abitibi greenstone belt

Otto van Breemen, K.B. Heather, and J.A. Ayer

2006

CURRENT RESEARCH

Natural Resources Canada Ressources naturelles Canada

Canada

©Her Majesty the Queen in Right of Canada 2006

ISSN 1701-4387
Catalogue No. M44-2006/F1E-PDF
ISBN 0-662-44362-4

A copy of this publication is also available for reference by depository libraries across Canada through access to the Depository Services Program's Web site at http://dsp-psd.pwgsc.gc.ca

A free digital download of this publication is available from GeoPub: http://geopub.nrcan.gc.ca/index_e.php

Toll-free (Canada and U.S.A.): 1-888-252-4301

Critical reviewer
Vicky McNicoll

Authors

O. van Breemen
(ovanbree@nrcan.gc.ca)
601 Booth Street
Ottawa, Ontario
K1A 0E8

K.B. Heather
(kevin.heather@antaresminerals.com)
Vice-President Geology
Antares Minerals Inc.
Casilla 730
La Serena, Chile

J.A. Ayer
(john.ayer@ndm.gov.on.ca)
Precambrian Geoscience Section
Ontario Geological Survey
933 Ramsey Lake Road
Sudbury, Ontario
Canada P3E 6B5

Publication approved by GSC Central Canada

Correction date:

All requests for permission to reproduce this work, in whole or in part, for purposes of commercial use, resale, or redistribution shall be addressed to: Earth Sciences Sector Information Division, Room 402, 601 Booth Street, Ottawa, Ontario K1A 0E8.

U-Pb geochronology of the Neoarchean Swayze sector of the southern Abitibi greenstone belt

Otto van Breemen, K.B. Heather, and J.A. Ayer

van Breemen, O., Heather, K.B., and Ayer, J.A., 2006: U-Pb geochronology of the Neoarchean Swayze sector of the southern Abitibi greenstone belt; Geological Survey of Canada, Current Research 2006-F1, 32 p.

Abstract: Precise U-Pb zircon geochronology of the Swayze greenstone belt reveals a 45 Ma history of volcanism with 19 ages ranging from 2739 Ma to 2695 Ma. Seven U-Pb ages demonstrate the coeval nature of regionally extensive 2.73 Ga iron-formation, which serves as a key stratigraphic marker correlative across major deformation zones. Age correlations are consistent with an upward-younging stratigraphic succession without major tectonic breaks or disruption, which can be correlated with equivalent stratigraphy across the southern Abitibi greenstone belt. The youngest volcanic rocks are interlayered with greywackes for which detrital zircons from two samples establish maximum ages of deposition of 2683 ± 6 Ma and 2695 ± 1 Ma. As the detrital zircon ages are mostly younger than 2704 Ma, the provenance of these sediments is inferred to be exclusively volcanic rocks of the immediately lower pile. Detrital zircons from the youngest sedimentary rocks, sandstone of the unconformable and fault-bounded Ridout Group, provide a maximum depositional age limit of 2688 ± 2 Ma. Older detrital zircon ages, in the 2742 to 2735 Ma range, are consistent with deeper erosional excavation of source rocks and more active tectonics at the time of deposition. The oldest plutonic rocks of 2.74 Ga are coeval with the oldest volcanic rocks recorded and no geochronological evidence for pre-existing basement has been found. Plutonism continued after cessation of extensive volcanism, including 2686 Ma to 2680 Ma syntectonic (D_2) granitoids and post-tectonic granitoids as young at 2.66 Ga. Titanite ages of 2615 ± 3 Ma to 2540 ± 4 Ma are interpreted in terms of crystal growth from late-stage fluids.

Résumé : La datation précise par la méthode U-Pb sur zircon de la ceinture de roches vertes de Swayze révèle une histoire volcanique d'une durée de 45 millions d'années établie d'après 19 âges U-Pb compris entre 2 739 Ma et 2 695 Ma. Sept âges U-Pb de 2,73 Ga révèlent le caractère concomitant d'une formation de fer d'étendue régionale, qui constitue un important repère stratigraphique permettant d'établir des corrélations entre les zones de déformation majeures. La corrélation des âges rend compte d'une succession stratigraphique devenant plus jeune vers le haut, sans discontinuité ni perturbation tectonique majeure, qu'il est possible de mettre en corrélation avec une stratigraphie équivalente dans la partie sud de la ceinture de roches vertes de l'Abitibi. Les roches volcaniques les plus récentes sont interstratifiées avec des grauwackes pour lesquels des zircons détritiques provenant de deux échantillons permettent d'établir des limites maximales d'âge de dépôt à 2 683 ± 6 Ma et à 2 695 ± 1 Ma. Puisque les âges des zircons détritiques sont généralement plus récents que 2 704 Ma, nous présumons que ces sédiments proviennent exclusivement des roches volcaniques de l'empilement immédiatement sous-jacent. Des zircons détritiques provenant des roches sédimentaires les plus récentes, des grès du Groupe de Ridout discordant et limité par des failles, permettent d'établir à 2 688 ± 2 Ma la limite maximale d'âge de dépôt. Les âges plus anciens des zircons détritiques, compris entre 2 742 et 2 735 Ma, vont dans le sens d'une érosion plus en profondeur des roches sources et d'une activité tectonique plus intense lors de la sédimentation. Les roches plutoniques les plus anciennes, datant de 2,74 Ga, sont contemporaines des plus anciennes roches volcaniques rapportées, et aucune preuve géochronologique n'a été trouvée permettant de démontrer l'existence d'un socle plus ancien. Le plutonisme s'est poursuivi après la fin de l'activité volcanique étendue et se matérialise, entre autres, par des granitoïdes syntectoniques (D_2) datant de 2 686 Ma à 2 680 Ma et des granitoïdes post-tectoniques aussi récents que 2,66 Ga. Des âges sur titanite s'échelonnant de 2 615 ± 3 Ma à 2 540 ± 4 Ma seraient la manifestation d'une croissance cristalline par des fluides tardifs.

INTRODUCTION

The Swayze granite-greenstone belt is the southwestern extension of the Abitibi greenstone belt, which is the largest greenstone belt in the world (700 km long by 300 km wide). The Swayze belt is connected to the southern Abitibi belt by narrow septa of volcanic-sedimentary rocks associated with the Porcupine Destor deformation zone and Ridout deformation zone that, respectively, wrap around the northern and southern margins of the Kenogamissi granitoid complex (Fig. 1). The Ridout deformation zone is likely the extension of the Cadillac Larder Lake deformation zone east of the southern Abitibi belt further east. The Swayze belt is bounded to the north by the Nat River granitoid complex, and to the south by the Ramsey-Algoma granitoid complex. To the west it is bounded by the Kapuskasing structural zone, which is now generally accepted as an east-verging thrust exposing an oblique crustal cross-section of the Wawa Subprovince (Percival and Card 1983; Percival 1986). Unlike the main Abitibi belt, which is rich in VMS and gold deposits, few such mineral deposits have been found in the Swayze belt. However, as the distinction of the Abitibi and Swayze greenstone belts as two separate belts is historical and not geological, the Swayze belt remains a prospective area for economic mineral deposits.

The Abitibi belt consists of a complex and diverse array of volcanic, sedimentary, and plutonic rock types typically metamorphosed only to greenschist and subgreenschist grade, but locally attaining amphibolite grade adjacent to large synvolcanic to syntectonic intrusions (Jolly, 1978; Heather, 1998, 2001). Volcanic rocks range in composition from

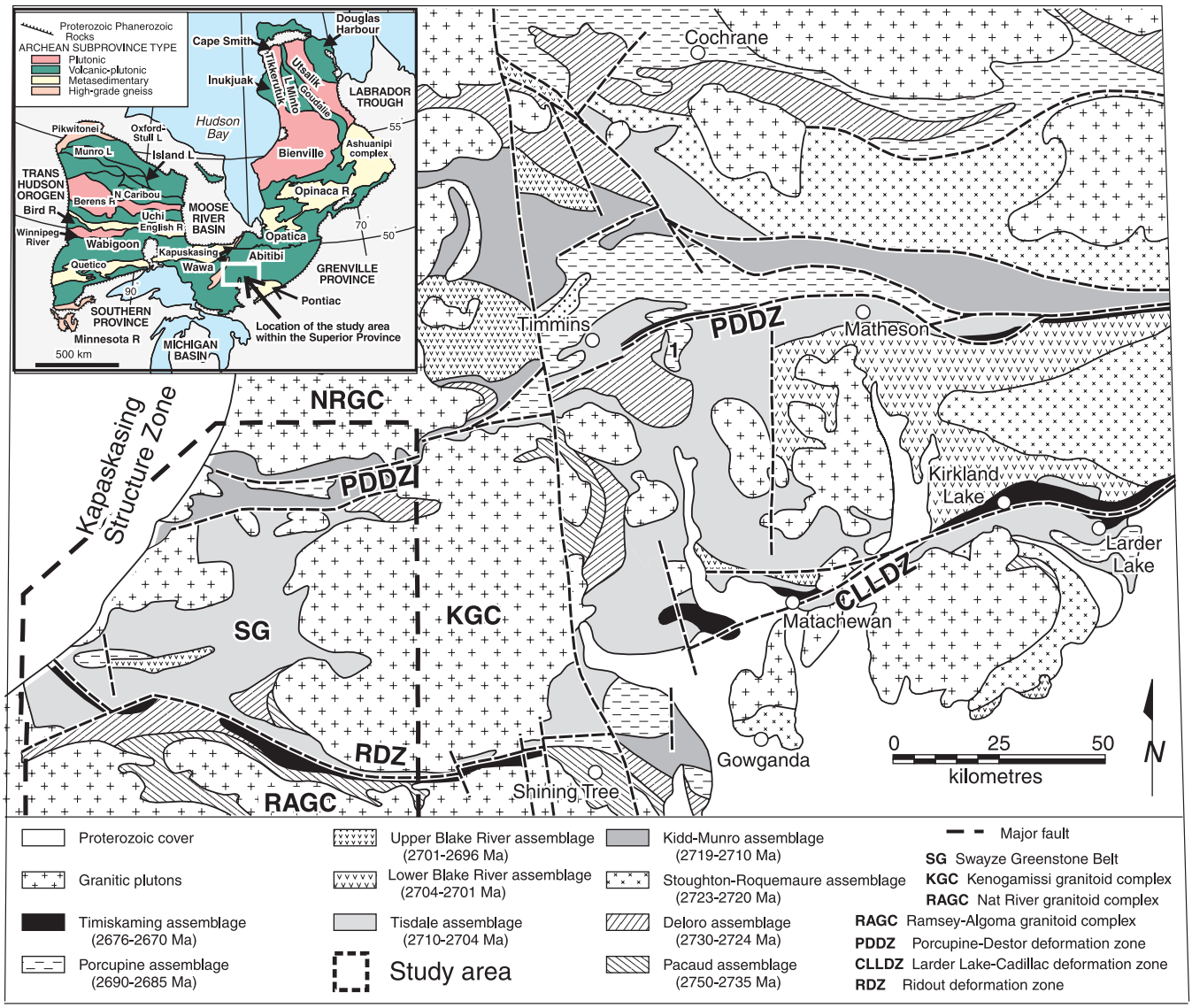

Figure 1. Regional geological sketch map of the southern Abitibi greenstone belt with assemblages after Ayer et al. (2002, 2005). The figure shows the separation of the Swayze greenstone belt from the main Abitibi greenstone belt by granitoid batholiths.

rhyolitic to komatiitic and commonly occur as mafic to felsic volcanic assemblages. Sedimentary rocks consist of both chemical and clastic varieties, and occur as both intra-volcanic sequences and as unconformably overlying sequences. A wide spectrum of plutonic rocks ranges from mafic to felsic in composition and they form large batholithic bodies to discrete stocks and dykes. Rocks of the Abitibi belt have undergone a complex sequence of deformation, ranging from early folding and faulting (possibly thrust faulting) through later upright folding, faulting, and ductile shearing. Throughout the Abitibi belt the development of large, dominantly east-west-trending, crustal-scale structures have created a lozenge-like pattern in the volcano-plutonic rock packages.

Heather (1998, 2001), on the basis of his systematic mapping and on the basis of preliminary geochronology, for which the full results are presented in this study, demonstrated a regular upward-facing 'layer cake' stratigraphy for the Swayze belt and suggested that the entire Abitibi belt may be a continuous belt within which there is correlative stratigraphy. Subsequently, in a broader study of the Abitibi belt, Ayer et al. (2002) demonstrated the existence of an autochthonous regional stratigraphy based on nine supracrustal assemblages. Further mapping and geochronology showed a coherent upward-facing section with about 20 per cent of the samples containing zircons with ages the same as those of the underlying assemblages (Fig. 1). The seven oldest assemblages represent semi-continuous volcanism from 2750 Ma to 2697 Ma. Autochthonous repetition of the different geodynamic environments resulted in five dominantly tholeitic±komatiitic assemblages and two dominantly calc-alkaline assemblages. A model of large-scale and long-lived interaction of mantle-plume- and subduction-related magmatism was proposed. The youngest two assemblages are dominantly sedimentary and were deposited unconformably on the volcanic rocks in proximity to regional faults. Recent refinements to the age ranges of the sedimentary assemblages in the Abitibi belt by Ayer et al. (2005) now reveal that the Porcupine assemblage consists of turbidite sequences with minor iron-formation and locally calc-alkaline felsic volcanic rocks deposited between 2690 Ma and 2685 Ma. The Timiskaming assemblage consists of subaerial conglomerate and fluvial sandstone locally with alkalic to shoshonitic volcanic rocks deposited between 2676 Ma and 2670 Ma. The sedimentary rocks are broadly contemporaneous with the emplacement of syntectonic plutonic rocks, regional deformation, and reactivation on regional faults. The latter activity is likely to have occurred during accretion of the Abitibi belt to the Superior Province Craton.

Ayer et al. (2002) also showed that the supracrustal rocks in the Swayze, Shining Tree, and Montcalm areas, which were originally considered to be distinct greenstone belts (Fig. 1), are, in fact, part of the southern Abitibi belt. This continuity of stratigraphy is not consistent with previous models of numerous supracrustal assemblages, or terranes, many of which were assumed to be tectonically superimposed (e.g. Jackson and Fyon, 1991). The object of this paper is to present TIMS (thermal-ionization mass spectrometry) isotope-dilution U-Pb geochronological data for the Swayze belt. It was this geochronology, underpinning detailed mapping, that led Heather and van Breemen (1994) and Heather et al. (1995) to propose a 'layer-cake' stratigraphy for the Swayze belt and started the rethinking of the tectonic architecture of the southern Abitibi belt. The U-Pb geochronology will be presented in two parts: 1) data that provide stratigraphic age control of supracrustal rocks, as well as information on the provenance of detrital zircons in sedimentary rocks, and 2) data that provide a temporal framework for the history of granitoid intrusion, providing constraints on the regional structure.

STRATIGRAPHY AND STRUCTURE

Like the rest of the Abitibi greenstone belt and greenstone belts elsewhere, the Swayze greenstone belt contains a diversity of both extrusive and intrusive rock types ranging from ultramafic through felsic in composition, as well as both chemical and clastic sedimentary rocks (Fig. 2, 3) (Heather 1998, 2001). Igneous rocks predominate and include both volcanic and plutonic rocks. The latter are found both internally in the supracrustal belts and externally, in large granitoid complexes. Sedimentary rocks occur mainly near the top of the succession. The area underwent a complex and protracted structural history of polyphase folding, development of multiple foliations, ductile high-strain zones and late brittle faulting. Several generations of penetrative foliation and folds (e.g. F_1, F_2, F_3, etc.), not necessarily multiple discrete episodes, have been identified based on overprinting relationships (Heather 1998, 2001).

The oldest penetrative deformation, D_1, consists of cryptically preserved penetrative foliation, contact high-shear zones associated with synvolcanic intrusions and isoclinal, commonly intrafolial folds. The map pattern preserved within the Swayze belt is dominated by regional F_2, and anticlines and synclines with an associated S_2 axial-planar foliation, interpreted to have formed during orogen-wide shortening across the entire Superior Province. The F_2 anticlines (e.g. Woman River anticline) tend to be open to tight, whereas the synclines (e.g. Brett Lake syncline) are tight to isoclinal (Fig. 2). The Ridout zone is a major east-west D_2 high-strain zone that is interpreted to be the western extension of the Larder Lake-Cadillac deformation zone of the Abitibi belt (Fig. 1, 2). A similar east-west structure, the Slate Rock high-strain zone is proximal to the northern margin of the Swayze belt and continues eastward into the Abitibi belt, where it is identified as the Porcupine-Destor deformation zone ((Fig. 1, 2). The D_2 event is synchronous with gold mineralization. Ubiquitous D_3 and D_4 deformations are associated with crenulation cleavage in high-strain zones and outcrop-scale folds. The northeast-striking Wakami high-strain zone is a prominent D_3 feature (Fig. 2).

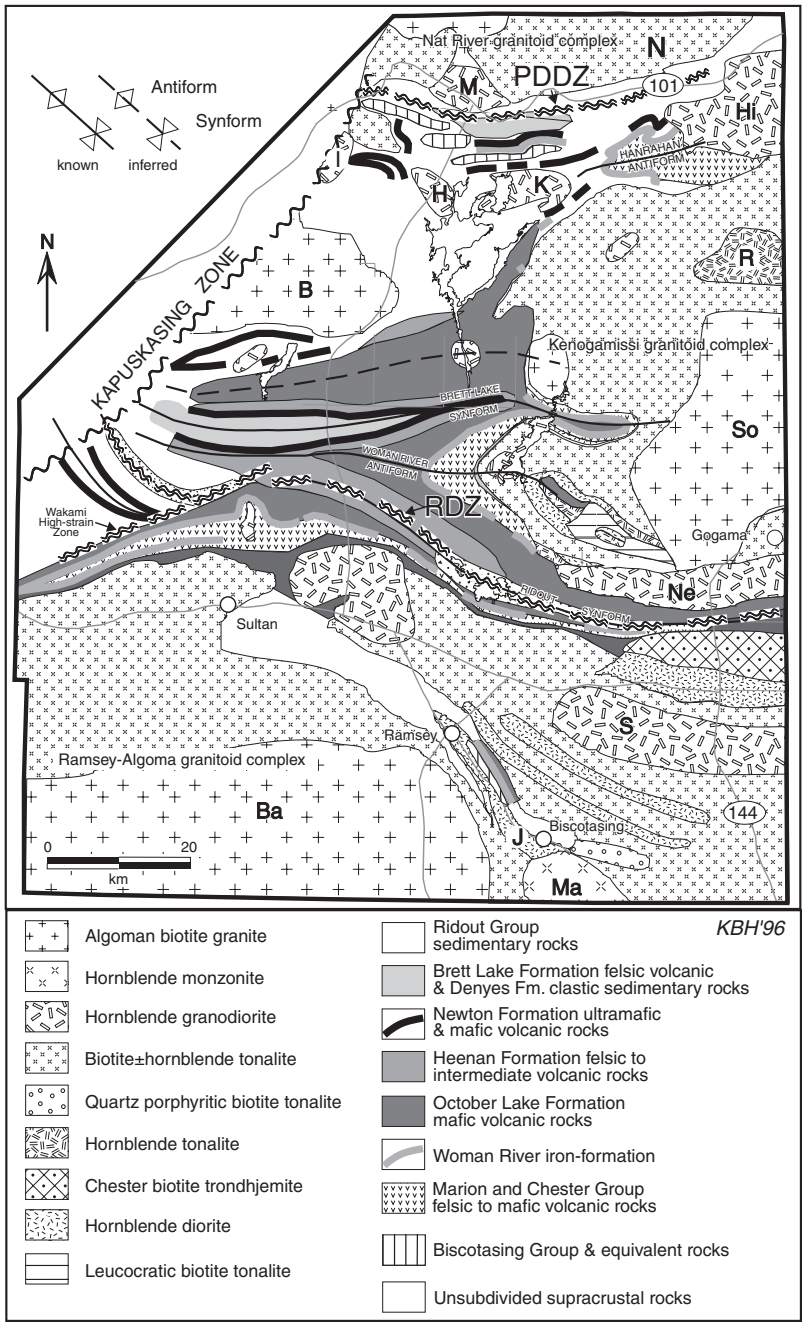

Figure 2. Geological sketch map of the Swayze greenstone belt after Heather (2001). Individual plutons are outlined for: I, Ivanhoe Pluton; M, Muskego Pluton; N, Nat River Pluton; H, Hoodoo Pluton; K, Kukatush Pluton; Hi, Hillary Pluton; Ne, Neville Pluton; S, Smuts Pluton; So, Somme Pluton; B, Biggs Pluton; Ba, Bardney Lake Batholith; J, Joffre Pluton; Ma, Margaret stock; R, Regan hornblende tonalite.

Heather et al. (1995) and Heather (1998) proposed a stratigraphy for the Swayze belt based on the recognition of a coherent, consistently upward-facing panel of rocks preserved on the north limb of the F_2 Woman River anticline (Fig. 2, 3b). This central, low-strain domain where primary stratigraphic and deposition relationships are relatively undisturbed is interpreted to be the result of a regional strain-shadow effect created by the Kenogamissi granitoid complex (Fig. 2). There is no evidence for significant early deformation in the form of old-over-young relationships or repetition or out-of-sequence rock units. The type section and additional reference sections at other key localities in the Swayze belt are also shown in Figures 3a and b. Stratigraphic reconstruction in the areas to the north and south of the type section is, unfortunately, hampered by increased strain, scarcity of marker units, the discontinuous nature of primary volcanic units due to rapid facies changes related to volcanic centres, and the possibility of nondeposition of specific volcanic and sedimentary horizons.

Heather et al. (1995) and Heather (2001) recognized six supracrustal groups (Fig. 3); from the oldest to the youngest these are the Chester, Marion, Biscotasing, Trailbreaker, Swayze, and Ridout groups. The Biscotasing Group, while present in the northern and the southern Swayze belt, is not found in the central Swayze belt (Fig. 3). These groups have

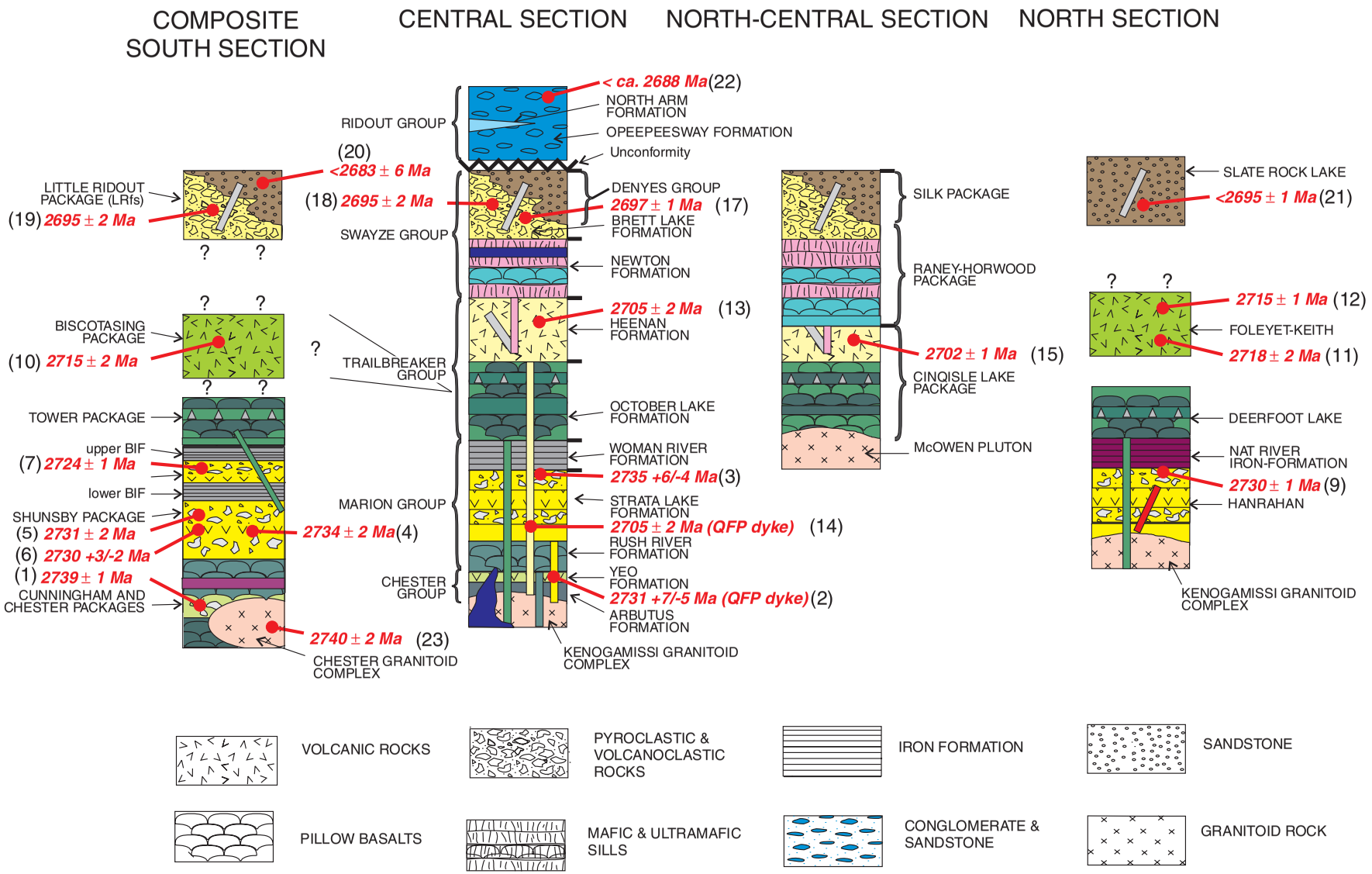

Figure 3a. Schematic sections for the Swayze greenstone belt after Heather (2001) showing with U-Pb zircon ages (BIF, banded iron-formation); RDZ, Ridout deformation zone; PDDZ, Porcupine Destor deformation zone. Colours identify units that can be correlated.

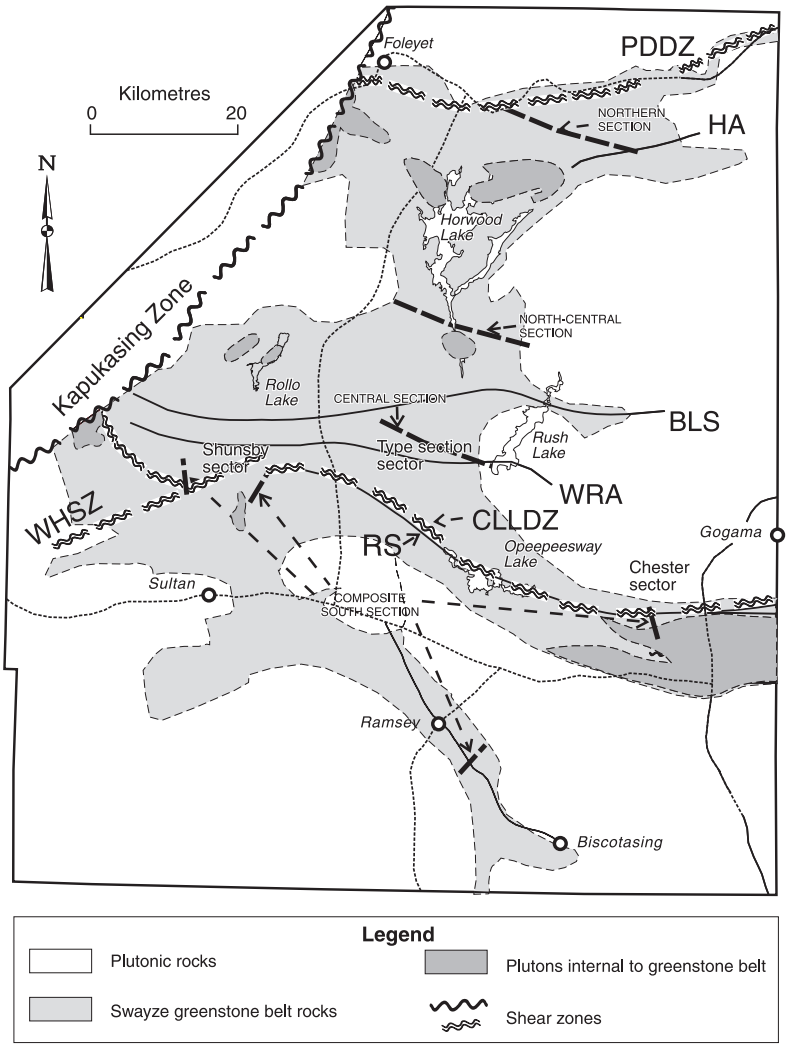

Figure 3b. Map showing locations of stratigraphic sections (RS, Ridout syncline; WRA, WomanRiver anticline; BLS, Brett Lake syncline; HA, Hanrahan anticline; WHSZ, Wakami high-shear zone). Legend the same as Figure 2.

subsequently been correlated with coeval assemblages having similar characteristic features across the southern Abitibi greenstone belt, respectively named the Pacaud, Deloro, Kidd-Munro, Tisdale and Blake river assemblages by Ayer et al. (2002) (Fig. 1). The highest stratigraphic level of the supracrustal sections is made up of clastic rocks and these are subdivided into two major types: an older sequence associated and intercalated with the volcanic rocks of the Swayze Group, and the younger Ridout Group that unconformably overlies the older volcanic and sedimentary rocks.

The most distinctive stratigraphic markers are the regionally extensive iron-formations (a major historical source of iron ore in the Abitibi belt) that can be mapped throughout the Swayze belt and are common within the Marion Group. Although not all the iron-formation bodies are the same age, there is a structurally disconnected, but regionally extensive, iron-formation that caps circa 2730 Ma felsic to intermediate volcanic rocks of this group. This horizon of iron-formation appears to be a time marker, if not a time-stratigraphic marker, that can be correlated across major deformation zones within the Swayze belt and likely across the Abitibi belt.

GEOCHRONOLOGY OF SUPRACRUSTAL ROCKS

This section presents the U-Pb zircon age results of 14 volcanic and hypabyssal rock samples that directly date stratigraphy in the Swayze belt, four crosscutting porphyries that yield minimum stratigraphic ages, and detrital zircons from three sandstone samples that yield maximum depositional ages. Sample locations for supracrustal rocks are shown in Figure 4. The age distribution of detrital zircons furthermore contributes to the understanding of the tectonic setting of the sedimentary basins. In addition, inherited zircons within the volcanic rocks yield information on the deeper rocks sampled by the ascending extrusive magmas. The stratigraphic position of samples investigated can be related to the four sections shown on Figure 3a and b: 1) a composite southern section, 2) a central or 'type' section across the Woman River anticline, 3) a north-central section, and 4) a northern section that crosses the Hanrahan anticline. For more complete geological information, the reader is referred to Heather (1998) and Heather (2001). Ages presented in this paper were previously

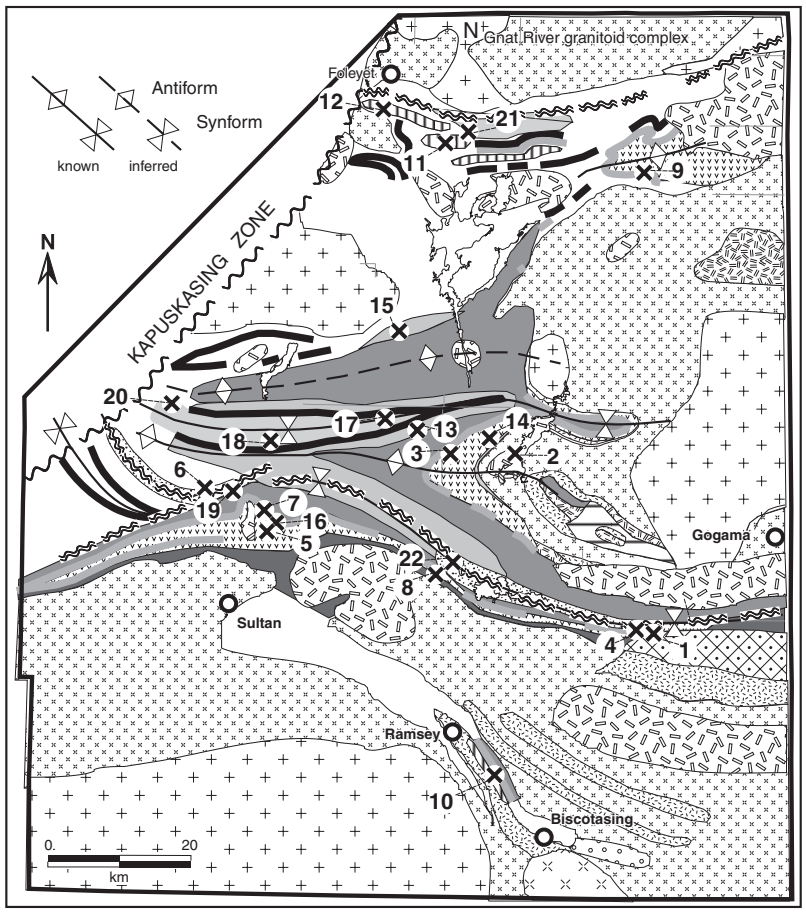

Figure 4. Map of the Swayze greenstone belt showing geochronology sample locations for supracrustal rocks. Legend the same as Figure 2.

reported in an Open File publication by Heather and Shore (1999). These preliminary ages and uncertainties are superseded by interpretations in this report.

Details of analytical techniques are given in Appendix I. U-Pb isotopic results and interpretations for volcanic rocks are presented in Tables 1 and 2, while those for plutonic rocks are presented in Tables 3 and 4. Uranium contents of zircons are consistently low; most are below 150 ppm (Tables 1 and 3). U-Pb isotopic results are displayed in concordia diagrams (Fig. 5–10). Besides age interpretations, Tables 2 and 4 provide details of stratigraphic information. They also include ages for which the data is published elsewhere. For both volcanic and plutonic rocks, the geochronology is discussed in order of decreasing age.

Zircon morphology and zoning is generally simple prismatic and characteristic of crystals growing in a melt. Only special features or deviations from this morphology are mentioned in the text. For volcanic and intrusive rocks, fractions are mostly multigrain with a median of 10 grains. Ages that predate crystallization reflect a mixture of ages of grains that are inherited and grains that grew during crystallization. These ages are, therefore, also mixed and cannot be attributed directly to the age of a specific source or stratigraphic horizon (cf. Heather, 1998). For the three sedimentary rocks investigated, however, all analyses are of single grains.

Chester Group

The oldest rocks found to date in the Swayze belt are assigned to the Chester Group, exposed in the core of the Woman River anticline. This group includes 1) mafic volcanic rocks and amphibolite of the Arbutus formation, and 2) the overlying intermediate volcanic rocks with associated minor sedimentary rocks and iron-formation of the Yeo Formation (Fig. 3a). Both formations are highly disrupted by the younger diorite and tonalite intrusions of the Kenogamissi granitoid complex and the synvolcanic 2.74 Ga Chester granitoid complex (*see* below). Ayer et al. (2002) correlated the Chester Group with the 2750 to 2735 Ma Pacaud assemblage, which comprises the oldest volcanic rocks in the southern Abitibi belt.

A felsic lapilli tuff (sample 1) was collected from the Yeo Formation in the Chester sector, southeastern Swayze belt (Fig. 3, 4). The sample contains acicular prismatic zircons with fluid inclusions that appear to fill negative crystals. As these inclusions extend the length of the grains, it is unlikely that the zircons contain inherited cores. These zircons yield an age of 2739 ± 1 Ma based on an upper concordia intersection of a four-point regression line (Fig. 5).

Table 1. U-Pb geochronological data for supracrustal rocks

Fraction[1]	Weight[2] µg	U ppm	Pb[3] ppm	$^{206}Pb/^{204}Pb$[4]	Pb[5] pg	$^{208}Pb/^{206}Pb$[6]	$^{207}Pb/^{235}U$[6]	$^{206}Pb/^{238}U$[6]	$^{207}Pb/^{206}Pb$[6]	$^{207}Pb/^{206}Pb$[7]	Disc[8]
1) Yeo Formation, felsic lapilli tuff (95-HNB-0277; Z4283; 47.5723°N 81.9695°E)											
A1, N0, 50	10	94	59	8378	4	0.19	13.675 ± 0.10	0.5231 ± 0.09	0.18961 ± 0.03	2739 ± 1	1.19
A2, N0, 50	13	55	34	5014	5	0.19	13.729 ± 0.11	0.5250 ± 0.10	0.18966 ± 0.03	2739 ± 1	0.84
B2, N0, 50	8	99	61	4354	6	0.17	13.830 ± 0.11	0.5290 ± 0.10	0.18960 ± 0.04	2739 ± 1	0.06
C1, N0, 50	12	52	32	2762	7	0.19	13.673 ± 0.12	0.5227 ± 0.11	0.18971 ± 0.05	2740 ± 2	1.29
2) Strata Lake porphyry (95-HNB-1121; Z4356; 47.7817°N 82.2569°E)											
A, N2, 40	4	79	47	469	24	0.12	13.711 ± 0.21	0.5259 ± 0.16	0.18908 ± 0.13	2734 ± 4	0.45
B, N2, 50	6	49	28	1338	7	0.08	13.521 ± 0.17	0.5206 ± 0.17	0.18836 ± 0.06	2728 ± 2	1.17
C, N2, 60	3	51	30	445	12	0.11	13.786 ± 0.29	0.5307 ± 0.28	0.18839 ± 0.13	2728 ± 4	-0.74
D, N2, 80	4	135	79	1756	11	0.1	13.882 ± 0.12	0.5285 ± 0.12	0.19049 ± 0.05	2746 ± 2	0.50
E, N2, 50	7	74	41	2861	6	0.1	13.048 ± 0.13	0.5059 ± 0.12	0.18706 ± 0.04	2717 ± 2	3.47
F, na	8	141	80	4613	8	0.1	13.268 ± 0.10	0.5135 ± 0.09	0.18740 ± 0.03	2720 ± 1	2.15
G, na	9	46	27	1282	11	0.1	13.490 ± 0.20	0.5197 ± 0.19	0.18826 ± 0.05	2727 ± 2	1.30
3) Strata Lake Formation, felsic volcanic breccia (94HNB-0059a; Z3716; 47.7773°N 70.3604°E)											
A, N1, 100	16	37	23	1883	11	0.14	14.033 ± 0.12	0.5318 ± 0.11	0.19138 ± 0.05	2754 ± 2	0.23
B, N1, 60	25	62	37	3179	16	0.14	13.696 ± 0.10	0.5215 ± 0.09	0.19047 ± 0.05	2746 ± 2	1.81
C, N1, 60	37	122	73	16063	9	0.13	13.589 ± 0.10	0.5231 ± 0.08	0.18843 ± 0.03	2729 ± 1	0.73
D, N1, 40	7	137	81	4570	6	0.13	13.510 ± 0.10	0.5209 ± 0.09	0.18811 ± 0.03	2726 ± 1	1.02
E, N1, 40	15	83	50	7641	5	0.16	13.765 ± 0.15	0.5267 ± 0.14	0.18953 ± 0.03	2738 ± 1	0.47
F, N1, 60	5	80	47	1595	8	0.13	13.384 ± 0.14	0.5183 ± 0.13	0.18727 ± 0.04	2718 ± 2	1.18
H, N1, 60	6	101	59	4816	1	0.12	13.600 ± 0.10	0.5233 ± 0.09	0.18848 ± 0.03	2729 ± 1	0.70
I, N1, 100	4	127	75	2556	6	0.13	13.477 ± 0.11	0.5198 ± 0.10	0.18803 ± 0.04	2725 ± 1	1.20
J, N1, 100	4	51	32	593	11	0.17	14.041 ± 0.19	0.5328 ± 0.16	0.19115 ± 0.10	2752 ± 3	-0.04
4) Strata Lake Formation, felsic lapilli tuff (95-HNB-0276; Z4134; 47.5647°N 81.9659°E)											
A, N0, 62-105	16	129	79	7434	9	0.18	13.567 ± 0.10	0.5226 ± 0.08	0.18828 ± 0.03	2727 ± 1	0.77
B, N0, 62-105	20	130	80	12881	6	0.17	13.762 ± 0.10	0.5262 ± 0.08	0.18970 ± 0.03	2740 ± 1	0.64
C, N0, 62-105	15	78	41	4791	7	0.17	11.269 ± 0.10	0.4575 ± 0.09	0.17866 ± 0.03	2641 ± 1	9.63
D, N0, 62-105	15	116	71	11058	0	0.17	13.723 ± 0.10	0.5268 ± 0.09	0.18894 ± 0.03	2733 ± 1	0.22
E, N2, 62-105	7	89	54	1666	12	0.15	13.837 ± 0.11	0.5285 ± 0.09	0.18990 ± 0.05	2741 ± 2	0.28
F, N2, 62-105	7	77	48	2300	8	0.18	13.702 ± 0.11	0.5246 ± 0.10	0.18941 ± 0.04	2737 ± 1	0.82
5) Strata Lake Formation, felsic lapilli tuff (93HNB0087a; Z3297; 47.7033°N 82.6586°E)											
B, M, 50	7	49	30	883	13	0.18	13.677 ± 0.22	0.5251 ± 0.21	0.18891 ± 0.08	2733 ± 3	0.54
C, M, 60	25	43	27	4306	7	0.19	13.713 ± 0.13	0.5270 ± 0.12	0.18873 ± 0.04	2731 ± 1	0.10
D, M, 80	24	49	31	947	43	0.18	13.695 ± 0.16	0.5265 ± 0.11	0.18866 ± 0.11	2731 ± 4	0.17
6) Strata Lake Formation, felsic crystal tuff (95-HNB-0085; Z4281; 47.7308°N 82.7736°E)											
A, N5, 40-50	9	57	37	3668	4	0.26	13.732 ± 0.12	0.5276 ± 0.12	0.18875 ± 0.05	2731 ± 2	-0.01
B, N5, 75	10	17	11	2160	3	0.21	13.775 ± 0.22	0.5295 ± 0.21	0.18870 ± 0.07	2731 ± 2	-0.37
C, N5, 40-50	10	63	40	3151	7	0.22	13.629 ± 0.10	0.5248 ± 0.09	0.18834 ± 0.04	2728 ± 1	0.36
7) Strata Lake Formation, volcanoclastic rock (93HNB0205b; Z3280; 47.7192°N 82.6639°E)											
A, M, 70	7	76	47	1680	11	0.17	13.670 ± 0.12	0.5276 ± 0.11	0.18793 ± 0.06	2724 ± 2	-0.32
B, M, 100*	10	68	42	4061	6	0.16	13.637 ± 0.11	0.5263 ± 0.10	0.18793 ± 0.03	2724 ± 1	-0.08
C, M, 70	13	101	62	190	247	0.14	13.957 ± 0.46	0.5378 ± 0.14	0.18823 ± 0.39	2727 ± 13	-2.14
D, M, 60	11	114	67	2793	15	0.12	13.566 ± 0.11	0.5234 ± 0.10	0.18799 ± 0.04	2725 ± 1	0.51

[1]All fractions are zircon; N = non-magnetic at a side slope given in degrees on a Frantz isodynamic magnetic separator operating at 1.8 amps; Sizes (width) in µm before abrasion, na = not available, *single grain analysis
[2]error on weight = ±1 µg
[3]radiogenic Pb
[4]measured ratio corrected for spike and Pb fractionation of 0.09 ± 0.03 percent per AMU
[5]total common Pb on analysis corrected for fractionation and spike
[6]corrected for blank Pb and U, common Pb, errors quoted are one sigma in percent
[7]age errors quoted are 2 SE in Ma
[8]discordance in per cent along a discordia to origin

Table 1 (cont.)

Fraction[1]	Weight[2] µg	U ppm	Pb[3] ppm	$^{206}Pb/^{204}Pb$[4]	Pb[5] pg	$^{208}Pb/^{206}Pb$[6]	$^{207}Pb/^{235}U$[6]	$^{206}Pb/^{238}U$[6]	$^{207}Pb/^{206}Pb$[6]	$^{207}Pb/^{206}Pb$[7]	Disc[8]
8) Esther felspar-quartz porphyry (93HNB0063a; Z3460; 47.6525°N 82.3306°E)											
A, N2, 60-150*	7	79	45	5017	4	0.08	13.617 ± 0.11	0.5256 ± 0.10	0.18788 ± 0.03	2724 ± 1	0.03
B, N2, 70-100	22	105	60	8093	9	0.09	13.350 ± 0.10	0.5170 ± 0.09	0.18729 ± 0.03	2719 ± 1	1.44
C, N2, 40-70	10	92	54	2431	12	0.13	13.440 ± 0.11	0.5191 ± 0.10	0.18776 ± 0.06	2723 ± 2	1.22
9) Strata Lake Formation, felsic lapilli tuff (93HNB-208; Z3802; 48.1361°N 82.0155°E)											
A, N2, 70	17	53	33	4906	1	0.19	13.732 ± 0.11	0.5278 ± 0.10	0.18868 ± 0.03	2731 ± 1	-0.07
D, N2, 60	30	49	31	9710	5	0.21	13.698 ± 0.10	0.5270 ± 0.09	0.18853 ± 0.03	2729 ± 1	0.03
10) Biscotasing Group, quartz-phyric flow (94-HNB-0267; Z3827; 47.4091°N 82.2525°E)											
B, N0, 40	6	100	59	1483	13	0.12	13.464 ± 0.14	0.5223 ± 0.13	0.18696 ± 0.05	2716 ± 2	0.30
C, N0, 30	8	107	63	875	31	0.13	13.458 ± 0.24	0.5210 ± 0.21	0.18735 ± 0.18	2719 ± 6	0.71
D, M0, 30	14	97	57	3478	13	0.12	13.355 ± 0.11	0.5185 ± 0.10	0.18681 ± 0.03	2714 ± 1	0.97
E, M0, 30	7	134	77	3377	9	0.1	13.408 ± 0.10	0.5198 ± 0.09	0.18707 ± 0.04	2717 ± 1	0.82
11) Biscotasing Group, quartz-phyric felsic volcanic rock (94-HNB-0281; Z3844; 48.1777°N 82.3730°E)											
A, N1, 70	3	65	38	1100	6	0.13	13.373 ± 0.25	0.5182 ± 0.25	0.18717 ± 0.07	2718 ± 2	1.17
B, N1, 70	4	245	144	8911	4	0.12	13.524 ± 0.10	0.5239 ± 0.09	0.18722 ± 0.03	2718 ± 1	0.10
C, N1, 60	5	311	183	12027	3	0.12	13.521 ± 0.10	0.5235 ± 0.09	0.18733 ± 0.03	2719 ± 1	0.22
12) Biscotasing Group, felsic flow breccia (94HNB-0285; Z3868; 48.2130°N 82.4584°E)											
A, N5, 62-74	9	90	55	3585	7	0.17	13.298 ± 0.10	0.5175 ± 0.09	0.18639 ± 0.03	2711 ± 1	1.00
B, N5, 62-74	10	65	38	2527	6	0.16	13.087 ± 0.14	0.5087 ± 0.14	0.18659 ± 0.04	2712 ± 1	2.76
C, N5, 62-74	11	87	53	2951	10	0.17	13.454 ± 0.12	0.5222 ± 0.11	0.18688 ± 0.03	2715 ± 1	0.29
D, N5, 62-74	8	71	44	2248	8	0.18	13.457 ± 0.12	0.5228 ± 0.11	0.18669 ± 0.05	2713 ± 2	0.10
E, N5, 62-74	10	32	20	1501	7	0.22	13.487 ± 0.14	0.5236 ± 0.13	0.18681 ± 0.05	2714 ± 2	-0.01
F, N5, 62-74	11	56	36	3967	5	0.25	13.486 ± 0.11	0.5233 ± 0.10	0.18691 ± 0.04	2715 ± 1	0.09
13) Heenan Formation, felsic volcanic rock (92-HNB-0087C; Z3025; 47.8016°N 82.3982°E)											
A, N1, 35	5	54	33	709	13	0.15	13.790 ± 0.38	0.5300 ± 0.38	0.18872 ± 0.09	2731 ± 3	-0.46
B, N1, 30	4	51	31	411	15	0.16	13.357 ± 0.58	0.5222 ± 0.55	0.18550 ± 0.19	2703 ± 6	-0.27
C, N1, 60	9	58	35	2805	6	0.14	13.761 ± 0.23	0.5259 ± 0.21	0.18977 ± 0.10	2740 ± 3	0.71
D, N1, 70	26	99	58	3110	26	0.13	13.099 ± 0.11	0.5127 ± 0.09	0.18529 ± 0.03	2701 ± 1	1.47
E, N1, 35-70	20	102	60	769	86	0.12	13.390 ± 0.15	0.5224 ± 0.11	0.18589 ± 0.09	2706 ± 3	-0.15
F, N1, 40	14	69	40	1594	19	0.15	12.784 ± 0.14	0.5018 ± 0.12	0.18479 ± 0.05	2696 ± 2	3.38
14) Heenan porphyry (95HNB-0258; Z4355; 47.7945°N 82.3010°E)											
E, N2, 40	4	34	19	437	10	0.09	13.261 ± 0.36	0.5203 ± 0.36	0.18486 ± 0.14	2697 ± 5	-0.15
A, N2, 50	8	71	40	1018	18	0.1	13.235 ± 0.14	0.5166 ± 0.11	0.18581 ± 0.07	2705 ± 2	0.93
F, N2, 40	6	95	54	678	27	0.09	13.332 ± 0.18	0.5205 ± 0.14	0.18578 ± 0.12	2705 ± 4	0.18
D, N2, 30	7	19	11	307	15	0.16	13.285 ± 0.35	0.5180 ± 0.31	0.18601 ± 0.19	2707 ± 6	0.75
G, N2, 70	4	145	83	2119	8	0.09	13.369 ± 0.15	0.5165 ± 0.14	0.18771 ± 0.04	2722 ± 1	1.69
C, N2, 50	6	21	13	325	13	0.17	13.636 ± 0.38	0.5215 ± 0.36	0.18963 ± 0.18	2739 ± 6	1.49
15) Heenan Formation, felsic volcanoclastic rock (92HNB-0083; Z3869; 47.9392°N 82.4158°E)											
B, N1, 50	19	58	35	6099	6	0.17	13.326 ± 0.11	0.5211 ± 0.10	0.18546 ± 0.03	2702 ± 1	-0.07
C, M1, 50	16	41	24	3100	7	0.13	13.299 ± 0.11	0.5202 ± 0.10	0.18542 ± 0.04	2702 ± 1	0.09
D, M1, 80*	9	20	12	762	8	0.2	13.307 ± 0.19	0.5212 ± 0.18	0.18516 ± 0.08	2700 ± 3	-0.21
E, M1, 90	16	44	26	2981	7	0.15	13.285 ± 0.11	0.5193 ± 0.10	0.18554 ± 0.04	2703 ± 1	0.30
16) Shunsby porphyry (93HNB0206b; Z3296; 47.7200°N 82.6633°E)											
B, N2, 50	15	90	52	4846	9	0.13	13.046 ± 0.12	0.5129 ± 0.11	0.18448 ± 0.03	2694 ± 1	1.11
C, N2, 40	15	121	69	8003	2	0.11	13.181 ± 0.11	0.5171 ± 0.10	0.18489 ± 0.03	2697 ± 1	0.48
D, N2, 30	4	90	52	1385	6	0.13	12.941 ± 0.16	0.5092 ± 0.14	0.18433 ± 0.08	2692 ± 3	1.78

Table 1 (cont.)

Fraction[1]	Weight[2] µg	U ppm	Pb[3] ppm	$^{206}Pb/^{204}Pb$[4]	Pb[5] pg	$^{208}Pb/^{206}Pb$[6]	$^{207}Pb/^{235}U$[6]	$^{206}Pb/^{238}U$[6]	$^{207}Pb/^{206}Pb$[6]	$^{207}Pb/^{206}Pb$[7]	Disc[8]
18) Brett Lake Formation, felsic ash (95HNB-0273; Z4354; 47.7987°N 82.6481°E)											
A, N2, 90	14	50	29	1028	22	0.13	13.188 ± 0.18	0.5181 ± 0.14	0.18462 ± 0.11	2695 ± 4	0.18
B, N2, 90	14	19	11	597	15	0.14	13.197 ± 0.29	0.5190 ± 0.24	0.18443 ± 0.19	2693 ± 6	-0.08
C, N2, 70	15	57	34	2415	12	0.13	13.165 ± 0.12	0.5172 ± 0.11	0.18460 ± 0.06	2695 ± 2	0.33
D, N2, 70	9	34	20	1242	8	0.14	13.189 ± 0.18	0.5182 ± 0.15	0.18461 ± 0.11	2695 ± 4	0.15
E, N2, 70	9	32	19	955	10	0.15	13.231 ± 0.21	0.5185 ± 0.18	0.18509 ± 0.12	2699 ± 4	0.29
F, N2, 40	16	43	25	2358	10	0.15	13.162 ± 0.12	0.5169 ± 0.10	0.18467 ± 0.06	2695 ± 2	0.42
19) Brett Lake Formation, felsic crystal tuff (95-HNB-0268; Z4282; 47.7222°N 82.7484°E)											
C, N0, 50	10	34	21	1598	7	0.21	13.179 ± 0.12	0.5177 ± 0.11	0.18463 ± 0.05	2695 ± 2	0.25
D, N0, 50	8	37	23	1419	7	0.21	13.208 ± 0.16	0.5186 ± 0.16	0.18470 ± 0.07	2696 ± 2	0.10
E, N0, 50	5	33	20	1282	4	0.19	13.237 ± 0.23	0.5200 ± 0.23	0.18462 ± 0.07	2695 ± 2	-0.20
G, M0, 30-40	15	54	34	4078	6	0.22	13.100 ± 0.10	0.5152 ± 0.09	0.18440 ± 0.03	2693 ± 1	0.63
F, M0, 30	10	53	33	2285	7	0.24	12.950 ± 0.13	0.5102 ± 0.12	0.18407 ± 0.05	2690 ± 2	1.46
20) Deynes Formation, sandstone (95-HNB-0206a1; Z4319; 47.8464°N 82.8067°E)											
B3, N-1, 60*	3	27	16	362	8	0.13	13.092 ± 0.81	0.5179 ± 0.82	0.18332 ± 0.18	2683 ± 6	-0.33
C6, N-1, 80*	5	21	12	708	4	0.11	12.901 ± 0.61	0.5068 ± 0.61	0.18463 ± 0.09	2695 ± 3	2.35
C4, N-1, 50*	3	17	10	534	3	0.14	13.016 ± 1.44	0.5111 ± 1.45	0.18472 ± 0.16	2696 ± 5	1.57
C1, N-1, 120*	3	40	23	387	11	0.14	12.536 ± 0.53	0.4908 ± 0.52	0.18526 ± 0.15	2701 ± 5	5.68
C2, N-1, 120*	7	32	20	969	8	0.16	13.562 ± 0.31	0.5254 ± 0.31	0.18721 ± 0.07	2718 ± 2	-0.19
C3, N-1, 200*	5	16	10	393	8	0.16	13.643 ± 0.84	0.5265 ± 0.85	0.18792 ± 0.15	2724 ± 5	-0.13
21) Deynes Formation, sandstone (94HNB-0287; Z3867; 48.1810°N 82.3589°E)											
H, N3, 80*	7	88	52	2879	7	0.13	13.235 ± 0.14	0.5199 ± 0.13	0.18463 ± 0.04	2695 ± 1	-0.18
B, N3, 70*	3	68	40	434	16	0.12	13.373 ± 0.26	0.5252 ± 0.22	0.18468 ± 0.15	2695 ± 5	-1.17
L, N3, 60*	5	59	35	2388	4	0.15	13.300 ± 0.25	0.5220 ± 0.24	0.18480 ± 0.05	2696 ± 2	-0.51
G, N3, 90*	7	65	38	3318	3	0.12	13.272 ± 0.18	0.5200 ± 0.17	0.18509 ± 0.04	2699 ± 1	-0.01
A, N3, 80*	4	67	39	1808	5	0.13	13.281 ± 0.17	0.5203 ± 0.17	0.18514 ± 0.06	2699 ± 2	-0.04
I, N3, 80*	10	103	60	6008	6	0.11	13.285 ± 0.12	0.5200 ± 0.11	0.18527 ± 0.03	2701 ± 1	0.06
K, N3, 70*	5	66	38	3281	3	0.12	13.161 ± 0.21	0.5151 ± 0.20	0.18529 ± 0.04	2701 ± 1	1.01
C, N3, 70*	4	50	30	1448	5	0.15	13.338 ± 0.22	0.5220 ± 0.22	0.18532 ± 0.08	2701 ± 3	-0.30
F, N3, 80*	6	33	19	1309	5	0.12	13.055 ± 0.36	0.5104 ± 0.36	0.18550 ± 0.08	2703 ± 3	2.00
E, N3, 110*	10	33	20	2017	5	0.13	13.616 ± 0.31	0.5281 ± 0.31	0.18701 ± 0.05	2716 ± 2	-0.78
22) Opeepeesway Formation, sandstone (93HNB-0067a; Z3649; 47.6599°N 82.3248°E)											
K, N3, 100*	7	70	42	2455	7	0.16	13.048 ± 0.12	0.5147 ± 0.11	0.18386 ± 0.05	2688 ± 2	0.51
G, N3, 100*	5	58	33	1501	5	0.12	13.160 ± 0.13	0.5139 ± 0.13	0.18571 ± 0.06	2705 ± 2	1.41
J, N3, 100*	6	44	27	1707	5	0.16	13.735 ± 0.15	0.5267 ± 0.12	0.18914 ± 0.05	2735 ± 2	0.32
I, N3, 100*	5	33	20	870	7	0.13	13.700 ± 0.22	0.5249 ± 0.18	0.18931 ± 0.09	2736 ± 3	0.74
D, N3, 150*	6	83	48	4336	4	0.09	13.830 ± 0.11	0.5297 ± 0.10	0.18936 ± 0.04	2737 ± 1	-0.16
L, N3, 100*	6	37	22	1820	4	0.12	13.839 ± 0.15	0.5299 ± 0.13	0.18942 ± 0.05	2737 ± 2	-0.17
C, N3, 150*	9	90	53	4284	5	0.11	13.856 ± 0.11	0.5301 ± 0.10	0.18960 ± 0.03	2739 ± 1	-0.13
B, N3, 200*	12	56	34	874	25	0.15	13.850 ± 0.14	0.5294 ± 0.11	0.18976 ± 0.08	2740 ± 3	0.06
E, N3, 130*	6	53	32	1379	8	0.13	13.957 ± 0.13	0.5330 ± 0.12	0.18994 ± 0.06	2742 ± 2	-0.55
H, N3, 100*	5	37	22	1749	3	0.13	13.868 ± 0.16	0.5294 ± 0.15	0.19001 ± 0.07	2742 ± 2	0.16

Table 2. Table summarizing ages, stratigraphic position, and geochronological details of volcanic and sedimentary rocks.

No.	Lab#	Field#	Age (Ma)	Rock type	Formal name	Group	Age interpretation	Geographic name
1	z4283	95HNB-277	2739 ± 1	felsic lapilli tuff	Yeo Formation	Chester	4 points, 0.1 - 1.3% disc.; UI = 2739.0 ± 0.6 Ma; LI forced through zero: MSWD = 0.40; POF = 67%.	Chester sector
2	z4356	95HNB-1121	2731 +7/-5	quartz porphyric felsic dyke	Strata Lake porphyry	_____	5 points, up to 3.5% disc; UI = 2731 +7/-5; LI = 0.8 ± 3 Ga; MSWD = 5.7, POF = 0.09%; slight inheritance in two points.	Type Section sector
3	z3716	94HNB-59a3	2735 +6/-4	quartz-eye felsic volcanic breccia	Strata Lake Formation	Marion	4 points, 0.7 - 1.2% disc.; UI = 2734.6 +5.8/-3.4; LI = 1.10 ± 3.7 Ga; MSWD = 0.18; POF = 83%; 3 discarded; 2 conc. 2753 Ma inheritance.	Type Section sector
4	z4134	95HNB-276	2734 ±2	felsic lapilli tuff	Strata Lake Formation	Marion	3 points, 0.2%, 0.8% and 9.6% disc; UI = 2734.0 +1.4/-1.4; LI = 1179 ± 17 Ma; MSWD = 1.3, POF = 26%; ; 3 analyses interpreted to be inherited.	Chester sector
5	z3297	93HNB-87a2	2731 ± 2	felsic lapilli tuff	Strata Lake Formation	Marion	3 points, conc. to 0.5% discordant; weighted average = 2731.2 ± 1.1 Ma; MSWD = 0.70; POF = 50%.	Shunsby sector
6	z4281	95HNB-85	2730 +3/-2	felsic feldspar crystal tuff	Strata Lake Formation	Marion	3 points, conc. to 0.4% discordant; UI = 2730.2 +2.9/-1.8; MSWD = 1.5; POF = 22%; LI = 1.06 ± 0.65 Ga.	Shunsby sector
7	z3280	93HNB-205b	2724 ± 1	felsic volcanoclastic	Strata Lake Formation	Marion	3 points, conc. to 0.5% disc.; UI = 2724.3 ± 0.8; LI forced through zero; MSWD = 0.2, POF = 65%.	Shunsby sector
8	z3460	93HNB-63a	2724 +4/-3	feldspar-quartz porphyry dyke	Esther FQP	_____	3 points, conc. to 1.4% disc.; UI = 2724.1 +4.1/-2.8 Ma; LI = 0.70 ± 0.42 Ga; MSWD = 5.6; POF = 1.8%.	Chester sector
9	z3802	93HNB-208a2	2730 ± 1	felsic lapilli tuff	Strata Lake Formation	Marion	2 points, conc.; weighted average = 2729.9 ± 0.7; MSWD = 3.35; POF = 7%.	Northern Swayze (Hanrahan package)
10	z3827	94HNB-267	2715 ± 2	quartz-phyric felsic flow	Biscotasing Group	Biscotasing	4 points, 0.3% to 1.0% disc; UI = 2715.4 ± 1.3; LI forced through zero; MSWD = 3.1, POF = 4.4%;	Biscotasing package
11	z3844	94HNB-281	2718 ± 2	quartz-phyric felsic volcanic	Biscotasing Group	Biscotasing	3 points, conc. to 1.2 % disc.; UI = 2718.5 +1.8/-1.1; LI = 0.14 ± 0.90 Ga; MSWD = 2.2; POF = 14%.	Northern Swayze (Keith package)
12	z3868	94HNB-285	2715 ± 1	felsic flow breccia	Biscotasing Group	Biscotasing	4 points, conc to 0.3% disc.; weighted average = 2714.7± 1.2; MSWD = 1.4 ; POF = 25%	Northern Swayze (Foleyet package)
13	z3025	92HNB-87c2	2705 ± 2	felsic volcanic	Heenan Formation	Trailbreaker	4 points, conc. to 3.4% disc.; UI = 2704.6 +2.0/-1.8; LI = 0.51 ± 0.14 Ga; MSWD = 0.56; POF = 57%; 2 inherited points 2740 - 2730 Ma.	Type Section sector
14	z4355	95HNB-258	2705 ± 2	quartz porphyric felsic intrusion	Heenan Porphyry	_____	3 points, conc. to 0.9% disc.; weighted average = 2705.5 ± 2.0; MSWD = 0.17 ; POF = 84%; 2 slightly older points, one younger.	Type Section sector
15	z3869	92HNB-83a4	2702 ± 1	felsic volcanoclastic rock	Heenan Formation	Trailbreaker	4 points, conc to 0.3% disc; weighted average = 2702.2 ± 0.7; MSWD = 1.9, POF = 12.5%.	Central Swayze (Horwood sector)
16	z3296	93HNB-206b	2699 +3/-2	quartz-feldspar porphyry	Shunsby QFP dyke	_____	3 points, 0.5 % to 1.8 % discordant; UI = 2699 +2.8/-2.0 Ma; LI = 0.8 ± 0.3 Ga; MSWD = 1.1; POF = 29 %.	Shunsby Sector (Cunningham)
17			2697 ±1	felsic volcaniclastic sediment	Brett Lake Formation	Swayze	U-Pb TIMS on zircon (Cattell et al. 1984).	Type Section sector
18	z4354	95HNB-273	2695 ± 2	felsic ash/crystal tuff	Brett Lake Formation	Swayze	6 points, conc. to 0.4% disc.; weighted average = 2695.3 ± 1.2; MSWD = 0.88; POF = 49%.	Type Section sector
19	z4282	95HNB-268	2695 ± 2	felsic crystal tuff/ volcanoclastic sandstone	Brett Lake Formation	Swayze	5 points, conc. to 1.5 % disc.; UI = 2695.3 +1.7/-1.3; LI = 0.7 ± 0.3 Ga; MSWD = 0.29; POF = 83%.	Shunsby sector
20	z4319	95HNB-0206a1	<2683 ± 6	sandstone	Denyes Formation	Swayze	<2683 ± 6 Ma based on 1conc. point; 2724 Ma, 2718 Ma; 5 between 2704 Ma and 2695 Ma.	Western Swayze
21	z3867	94HNB-0287	<2695 ± 1	sandstone	Denyes Formation	Swayze	<2695 ± 1 Ma based on 2 conc. points; 2716 Ma and 9 between 2703 Ma and 2695 Ma.	Northern Swayze (Slate Rock Lake package)
22	z3649	93HNB-0067a	<ca. 2688	sandstone	Opeepeesway Formation	Ridout	<2688 ± 2 Ma based on 1 point 0.5% disc.	South Section (Ridout high-strain zone)

MSWD = mean square of weighted deviates; POF = probability of fit; UI (LI) = upper (lower) intercept age calculated from discordia regression line; conc. = concordant; disc. = discordant.

Table 3. U-Pb geochronological data for plutonic rocks.

Fraction[1]	Weight[2] µg	U ppm	Pb[3] ppm	$^{206}Pb/^{204}Pb$[4]	Pb[5] pg	$^{208}Pb/^{206}Pb$[6]	$^{207}Pb/^{235}U$[6]	$^{206}Pb/^{238}U$[6]	$^{207}Pb/^{206}Pb$[6]	$^{207}Pb/^{206}Pb$[7]	Disc[8]
23) Chester trondhjemite (92-HNB-0070C; Z2834; 47.5393°N 81.9447°E)											
A, N2, 65	10	97	59	3296	10	0.14	13.827 ± 0.12	0.5286 ± 0.11	0.18973 ± 0.03	2740 ± 1	0.20
B, N2, 40	12	47	29	801	23	0.15	13.914 ± 0.21	0.5323 ± 0.17	0.18960 ± 0.12	2739 ± 4	-0.56
C, N2, 40	4	40	25	1133	5	0.18	13.766 ± 0.54	0.5265 ± 0.54	0.18963 ± 0.07	2739 ± 2	0.54
D, N2, 50	19	72	43	400	115	0.15	13.657 ± 0.23	0.5234 ± 0.11	0.18924 ± 0.17	2736 ± 6	0.98
24) Gowgama tonalite, gneissic phase (95-HNB-0274a1; Z4168; 47.7015°N 81.7328°E)											
A, N-0.5, 62-105	22	96	55	1755	41	0.08	13.769 ± 0.11	0.5283 ± 0.08	0.18902 ± 0.05	2734 ± 2	-0.03
B, N-0.5, 62-105	15	109	62	11623	5	0.08	13.562 ± 0.11	0.5240 ± 0.10	0.18773 ± 0.03	2722 ± 1	0.29
C, N-0.5, 62-105	22	110	63	11214	7	0.07	13.615 ± 0.10	0.5244 ± 0.08	0.18831 ± 0.03	2728 ± 1	0.44
D, N-0.5, 62-105	6	45	26	952	10	0.07	13.583 ± 0.14	0.5245 ± 0.13	0.18784 ± 0.06	2723 ± 2	0.24
25) Biscotasing tonalite (94-HNB-1227A; Z3924; 47.3417°N 81.9934°E)											
A, N0, 60	31	118	67	11351	10	0.08	13.308 ± 0.11	0.5176 ± 0.10	0.18646 ± 0.03	2711 ± 1	0.99
B, N0, 60	24	168	95	15290	9	0.08	13.416 ± 0.10	0.5211 ± 0.08	0.18673 ± 0.03	2714 ± 1	0.44
C, N0, 60	38	153	87	1391	138	0.08	13.397 ± 0.11	0.5204 ± 0.08	0.18670 ± 0.06	2713 ± 2	0.56
D, N0, 60	31	163	92	28122	6	0.08	13.367 ± 0.10	0.5196 ± 0.08	0.18657 ± 0.03	2712 ± 1	0.66
26) Regan tonalite (92-HNB-0017A2; Z2837; 48.0033°N 81.8794°E)											
A, N 0.5, 150*	23	49	29	2294	3	0.13	13.397 ± 0.11	0.5214 ± 0.11	0.18635 ± 0.04	2710 ± 1	0.24
B, N0.5, 130*	25	56	34	4144	11	0.14	13.459 ± 0.10	0.5228 ± 0.09	0.18672 ± 0.03	2714 ± 1	0.12
C, N0.5, 90	31	49	29	3659	14	0.15	13.446 ± 0.10	0.5224 ± 0.09	0.18669 ± 0.03	2713 ± 1	0.18
D, N0.5, 90	27	50	30	5457	8	0.16	13.506 ± 0.10	0.5241 ± 0.09	0.18690 ± 0.03	2715 ± 1	-0.07
E, N0.5, 120*	20	53	31	6300	5	0.11	13.431 ± 0.12	0.5220 ± 0.11	0.18660 ± 0.03	2712 ± 1	0.21
F, N0.5, 100*	9	56	36	1531	8	0.22	13.452 ± 0.18	0.5225 ± 0.18	0.18672 ± 0.05	2714 ± 2	0.17
27) Heenan porphyry (94-HNB-0115; Z4280; 47.6397°N 82.2030°E)											
E, N1, 40	12	70	44	4722	4	0.21	13.355 ± 0.10	0.5208 ± 0.09	0.18600±0.03	2707±1	0.21
F, N1, 40	12	24	15	1089	8	0.19	13.356 ± 0.13	0.5211 ± 0.12	0.18588±0.06	2706±2	0.09
28) Northrup tonalite (92-HNB-0124; Z2836; 48.0108°N 81.7807°E)											
A, N0.5, 60	13	113	65	1736	27	0.12	13.214 ± 0.11	0.5178 ± 0.09	0.18509 ± 0.05	2699 ± 2	0.41
B, N0.5, 50	13	128	73	1986	26	0.1	13.181 ± 0.11	0.5174 ± 0.09	0.18478 ± 0.04	2696 ± 1	0.38
C, N0.5, 70	15	114	66	538	104	0.12	13.248 ± 0.19	0.5186 ± 0.10	0.18526 ± 0.13	2701 ± 4	0.33
D, N0.5, 50	17	120	68	4170	16	0.09	13.178 ± 0.10	0.5168 ± 0.08	0.18495 ± 0.03	2698 ± 1	0.56
29) Nat River pluton, biotite granodiorite (94-HNB-0282; Z3923; 48.2133°N 82.2953°E)											
A1, N2, 70	10	67	40	5783	3	0.14	13.222 ± 0.10	0.5179 ± 0.09	0.18517 ± 0.03	2700 ± 1	0.43
B, N2, 74-90	19	75	43	4580	10	0.11	13.157 ± 0.12	0.5176 ± 0.11	0.18434 ± 0.05	2692 ± 2	0.14
C, N2, 80	8	76	43	6578	3	0.07	13.198 ± 0.12	0.5181 ± 0.11	0.18473 ± 0.03	2696 ± 1	0.21
D, na	61	32	19	10824	4	0.14	13.344 ± 0.10	0.5210 ± 0.09	0.18577 ± 0.03	2705 ± 1	0.08
E, na	37	62	36	13220	4	0.11	13.304 ± 0.10	0.5206 ± 0.09	0.18533 ± 0.03	2701 ± 1	-0.03
30) Isaiah Creek stock, biotite granodiorite (93HNB0142; Z3288; 47.7133°N 82.6986°E)											
A1, M, 50	9	87	48	942	27	0.09	12.813 ± 0.21	0.5063 ± 0.19	0.18353 ± 0.14	2685 ± 5	2.00
A2, N3, 74-105	28	187	98	3909	41	0.08	12.169 ± 0.10	0.4835 ± 0.09	0.18254 ± 0.03	2676 ± 1	6.04
B1, M, 70-90	11	129	68	1426	31	0.1	12.171 ± 0.21	0.4807 ± 0.20	0.18363 ± 0.05	2686 ± 2	7.00
B2, N3, 74-105*	23	152	83	3267	34	0.07	12.919 ± 0.10	0.5087 ± 0.08	0.18419 ± 0.04	2691 ± 1	1.81
C, N3, 70-105	51	56	32	1702	5	0.12	13.089 ± 0.12	0.5156 ± 0.11	0.18411 ± 0.06	2690 ± 2	0.45
E, N3, 74-105	48	130	72	5920	33	0.11	12.399 ± 0.12	0.4999 ± 0.11	0.17989 ± 0.03	2652 ± 1	1.76
F, N3, 74-105	38	203	102	2257	99	0.09	11.488 ± 0.11	0.4621 ± 0.09	0.18030 ± 0.04	2656 ± 1	9.35
31) Kenogaming felsic dyke (93HNB0009a; Z3429; 48.1765°N 81.9464°E)											
C, M, 60	26	61	36	8493	6	0.16	13.115 ± 0.11	0.5171 ± 0.09	0.18395 ± 0.03	2689 ± 1	0.09
D, M,60	22	69	41	5308	9	0.16	13.150 ± 0.10	0.5179 ± 0.09	0.18416 ± 0.03	2691 ± 1	0.02
32) Muskego diorite (94-HNB-0286; Z4322; 48.2508°N 82.3858°E)											
A1, N0, 150	19	71	44	6699	2	0.21	13.047 ± 0.10	0.5153 ± 0.09	0.18364 ± 0.03	2686 ± 1	0.31
A2, N0, 150	19	184	112	3625	31	0.21	12.941 ± 0.11	0.5108 ± 0.10	0.18374 ± 0.04	2687 ± 1	1.22
B1, N0, 150	18	75	47	5551	8	0.23	13.066 ± 0.10	0.5162 ± 0.09	0.18357 ± 0.03	2685 ± 1	0.10
B2, N0, 150	23	144	89	14273	8	0.21	13.042 ± 0.10	0.5153 ± 0.08	0.18355 ± 0.03	2685 ± 1	0.26

[1]Fractions are zircon except for T = titanite and M =monazite; N = non-magnetic at a side slope given in degrees on a Frantz isodynamic magnetic separator operating at 1.8 amps; Sizes (width) in µm before abrasion, na = not available, *single grain analysis
[2]error on weight = ± 1 µg
[3]radiogenic Pb
[4]measured ratio corrected for spike and Pb fractionation of 0.09 ± 0.03 percent per AMU
[5]total common Pb on analysis corrected for fractionation and spike
[6]corrected for blank Pb and U,common Pb, errors quoted are one sigma in percent
[7]age errors quoted are 2 SE in Ma
[8]discordance in per cent along a discordia to origin

Table 3 (cont.)

Fraction[1]	Weight[2] µg	U ppm	Pb[3] ppm	$^{206}Pb/^{204}Pb$[4]	Pb[5] pg	$^{208}Pb/^{206}Pb$[6]	$^{207}Pb/^{235}U$[6]	$^{206}Pb/^{238}U$[6]	$^{207}Pb/^{206}Pb$[6]	$^{207}Pb/^{206}Pb$[7]	Disc[8]
33) Smuts Pluton, biotite granodiorite (94HNB-1135a2; Z3918; 47.4712°N 82.0122°E)											
A, N1, 90	44	58	34	11073	7	0.13	13.037 ± 0.10	0.5130 ± 0.08	0.18433 ± 0.03	2692 ± 1	1.04
B, N1, 90	21	77	45	8793	5	0.13	13.254 ± 0.10	0.5183 ± 0.08	0.18546 ± 0.03	2702 ± 1	0.47
C, N1, 110	14	37	22	2048	8	0.13	13.492 ± 0.12	0.5232 ± 0.11	0.18704 ± 0.04	2716 ± 1	0.16
D, N1, 110*	10	63	36	2565	8	0.12	13.126 ± 0.11	0.5174 ± 0.10	0.18399 ± 0.04	2689 ± 1	0.05
E, N1, 110	15	49	28	4901	5	0.11	13.071 ± 0.10	0.5161 ± 0.09	0.18367 ± 0.03	2686 ± 1	0.16
F, N1, 60	11	86	50	9815	3	0.13	13.291 ± 0.10	0.5174 ± 0.09	0.18632 ± 0.03	2710 ± 1	0.99
G, N1, 70	42	63	37	9642	9	0.13	12.995 ± 0.10	0.5131 ± 0.08	0.18367 ± 0.03	2686 ± 1	0.74
35) Neville Pluton, hornblende granodiorite (92-HNB-0123; Z3023; 47.6128°N 81.9308°E)											
A, N0, 100	31	112	69	8252	14	0.21	12.931 ± 0.11	0.5127 ± 0.10	0.18291 ± 0.03	2680 ± 1	0.51
B, N0, 40-70	13	109	67	1343	35	0.2	13.066 ± 0.12	0.5163 ± 0.10	0.18356 ± 0.06	2685 ± 2	0.09
C, N0, 65	20	113	71	2152	34	0.24	13.032 ± 0.11	0.5160 ± 0.10	0.18318 ± 0.04	2682 ± 1	-0.01
36) Kukatush Pluton, hornblende monzonite (94-HNB-0283; Z4321; 48.1180°N 82.1731°E)											
A, N3, 50	11	121	79	2773	16	0.29	13.037 ± 0.10	0.5156 ± 0.09	0.18338 ± 0.04	2684 ± 1	0.14
B, N3, 50	9	108	71	3018	10	0.31	12.997 ± 0.11	0.5144 ± 0.10	0.18323 ± 0.06	2682 ± 2	0.31
D, N3, 50	5	67	43	1879	6	0.27	12.963 ± 0.12	0.5136 ± 0.12	0.18305 ± 0.06	2681 ± 2	0.39
37) Hillary Pluton, hornblende granodiorite (92-HNB-0125; Z3024; 48.2625°N 81.8051°E)											
A, N1, 100	12	121	74	4922	10	0.19	13.152 ± 0.11	0.5174 ± 0.10	0.18436 ± 0.03	2693 ± 1	0.20
B, N1, 60	9	105	55	1223	23	0.15	11.451 ± 0.14	0.4557 ± 0.12	0.18224 ± 0.06	2673 ± 2	11.33
C, N1, 60	15	130	79	10946	6	0.18	13.216 ± 0.10	0.5207 ± 0.09	0.18408 ± 0.03	2690 ± 1	-0.55
D, N1, 50-80	8	262	157	2411	26	0.19	12.787 ± 0.11	0.5075 ± 0.10	0.18276 ± 0.05	2678 ± 2	1.47
E, N1, 50-150	11	334	187	3935	27	0.18	11.997 ± 0.11	0.4785 ± 0.10	0.18186 ± 0.03	2670 ± 1	6.75
F, N1, 120	11	193	119	18706	3	0.22	12.948 ± 0.10	0.5131 ± 0.09	0.18304 ± 0.03	2681 ± 1	0.50
G, N1, 120	11	169	104	5968	10	0.21	12.875 ± 0.10	0.5102 ± 0.08	0.18302 ± 0.03	2680 ± 1	1.04
39) Joffre Pluton, hornblende quartz-diorite (94-HNB-0280; Z3917; 47.4295°N 82.2904°E)											
A, N0, 70	14	114	67	4647	11	0.17	12.766 ± 0.10	0.5083 ± 0.09	0.18214 ± 0.03	2673 ± 1	1.05
C, N0, 70	18	222	131	15328	8	0.18	12.709 ± 0.09	0.5058 ± 0.08	0.18221 ± 0.03	2673 ± 1	1.56
D, N0, 70	13	139	82	10128	4	0.16	12.793 ± 0.10	0.5095 ± 0.09	0.18210 ± 0.03	2672 ± 1	0.80
E (T), M, 100	129	90	79	535	738	0.82	12.623 ± 0.24	0.5050 ± 0.12	0.18131 ± 0.18	2665 ± 6	1.37
F (T), M, 90	127	79	72	1168	292	0.87	12.856 ± 0.19	0.5117 ± 0.17	0.18223 ± 0.07	2673 ± 2	0.43
G (T), M, 90	127	86	75	1347	275	0.79	12.818 ± 0.12	0.5107 ± 0.09	0.18203 ± 0.06	2671 ± 2	0.54
40) Margaret stock, hornblende monzonite (94-HNB-1286; Z3935; 47.2550°N 82.1594°E)											
A, na	12	140	86	5834	9	0.22	12.802 ± 0.10	0.5113 ± 0.08	0.18159 ± 0.03	2667 ± 1	0.24
B, na	12	117	71	7370	6	0.2	12.826 ± 0.10	0.5122 ± 0.09	0.18161 ± 0.03	2668 ± 1	0.07
C, na	12	104	63	5471	7	0.2	12.723 ± 0.10	0.5087 ± 0.09	0.18141 ± 0.03	2666 ± 1	0.68
T1 (T)	409	136	130	2104	892	0.99	12.786 ± 0.12	0.5108 ± 0.10	0.18155 ± 0.05	2667 ± 2	0.32
T2 (T)	281	134	127	2880	440	0.96	12.790 ± 0.10	0.5110 ± 0.09	0.18154 ± 0.04	2667 ± 1	0.28
T3 (T)	159	128	119	2129	322	0.93	12.810 ± 0.11	0.5118 ± 0.09	0.18153 ± 0.05	2667 ± 2	0.11
T4 (T)	143	102	96	1459	340	0.94	12.819 ± 0.13	0.5124 ± 0.10	0.18143 ± 0.06	2666 ± 2	-0.05
41) Somme Pluton, biotite granite (92-HNB-0026B; Z2835; 47.7797°N 81.9921°E)											
A, N5, 20-70	9	96	51	3209	0	0.12	11.628 ± 0.15	0.4732 ± 0.14	0.17820 ± 0.05	2636 ± 2	6.33
B, N5, 50	11	197	104	4395	15	0.14	11.469 ± 0.11	0.4691 ± 0.09	0.17731 ± 0.03	2628 ± 1	6.79
E, N5, 40	7	71	42	1077	15	0.14	12.903 ± 0.14	0.5118 ± 0.13	0.18284 ± 0.06	2679 ± 2	0.65
P, N5, 30	13	257	125	2659	34	0.14	10.116 ± 0.11	0.4313 ± 0.09	0.17010 ± 0.04	2559 ± 1	11.48
TA (T), 120	124	41	32	786	212	0.64	12.175 ± 0.15	0.5018 ± 0.09	0.17597 ± 0.10	2615 ± 3	-0.29
TB (T), 160	137	40	21	1264	136	0.1	11.511 ± 0.33	0.4887 ± 0.25	0.17083 ± 0.17	2566 ± 6	0.03
TC (T), 180	131	42	22	1047	157	0.15	10.847 ± 0.13	0.4578 ± 0.10	0.17187 ± 0.07	2576 ± 2	6.81
MX (M), 150*	9	20	13	315	19	0.32	11.586 ± 0.44	0.4913 ± 0.41	0.17103 ± 0.20	2568 ± 7	-0.41
MY (M), 140*	7	32	16	641	6	0.05	11.141 ± 0.34	0.4804 ± 0.33	0.16819 ± 0.12	2540 ± 4	0.50
MZ (M), 170*	13	25	14	574	17	0.15	11.708 ± 0.26	0.4925 ± 0.25	0.17241 ± 0.10	2581 ± 4	-0.03
42) Biggs Pluton, biotite granite-granodiorite (HNB-95-280; Z4191; 47.9542°N 82.7603°E)											
A, na	15	170	91	626	126	0.11	12.160 ± 0.18	0.4841 ± 0.09	0.18218 ± 0.13	2673 ± 4	5.79
B, na	15	289	152	5146	25	0.13	11.775 ± 0.27	0.4684 ± 0.27	0.18231 ± 0.04	2674 ± 1	8.88
C, na	8	437	229	4002	27	0.1	11.881 ± 0.10	0.4760 ± 0.09	0.18101 ± 0.04	2662 ± 1	6.90
D,	9	401	216	1479	76	0.1	12.292 ± 0.12	0.4898 ± 0.10	0.18200 ± 0.06	2671 ± 2	4.59

Table 4. Table summarizing ages, igneous types, and geochronological details of plutonic rocks.

No.	Lab#	Sample#	U-Pb Age (Ma)	Rock Type	Formal Name	Category	Statistics	Geographic Name
23	z2834	92HNB-70a3	2740 ± 2	biotite trondhjemite	Chester trondhjemite	Synvolcanic	4 points, -0.6 to 1.0% discordant; UI = 2739.8 +1.8/-1.1 Ma; LI = 0.37 ± 0.79 Ga; MSWD = 1.0; POF = 36%.	Chester granitoid complex
24	z4168	95HNB-274a1	2722 ± 1	hornblende-biotite tonalite gneiss	Gogama tonalite	Synvolcanic	2 points, concordant and 0.3% discordant, weighted average = 2722.5 ± 0.8 Ma; MSWD = 0.77; POF = 38 %; two inherited fractions 2734 ± 2 Ma and 2728 ± 1 Ma.	Kenogamissi granitoid complex
25	z3924	94HNB-1227a1	2715 +3/-2	biotite-hornblende tonalite	Biscotasing tonalite	Synvolcanic	4 points, 0.4 % to 1.0 % discordant; UI = 2715.3 +2.7/-1.8 Ma; LI = 0.79 ±0.38 Ga; MSWD = 0.26; POF = 77%.	Ramsey-Algoma granitoid complex
26	z2837	92HNB-17a2	2715 ± 2	hornblende tonalite	Regan tonalite	Synvolcanic	5 points, conc.; UI = 2714.6 +2.2/-1.0 Ma; LI = 1.2 ± 0.7 Ga; MSWD = 0.06; LI = POF = 100 %; one fraction with different Pb loss.	Kenogamissi granitoid complex
27	z4280	94HNB-115	2707 ± 1	intermediate crystal tuff (quartz-feldspar porphyry intrusion)	Heenan porphyry	Synvolcanic	2 points, conc, weighted average = 2706.9 ± 0.9; MSWD = 0.97, POF = 33%.	Trailbreaker group (Chester sector)
28	z2836	92HNB-124a	2698 ± 1	biotite tonalite	Northrup tonalite	Synvolcanic	4 points, 0.3 % to 0.6 % disc.; weighted average = 2697.7 ± 0.8; MSWD = 2.8; POF = 4.1.	Kenogamissi granitoid complex
29	z3923	94HNB-0282	<2692 ± 2	biotite granodiorite	Nat River pluton (Muskego granodiorite)	Group I transitional	<2692 ± 2 Ma based on one conc. point; scatter of 4 points, conc to 0.4 % discordant; 2705.1 to 2692.3 ± 1.61.	Nat River granitoid complex
30	z3288	93HNB-142a2	<2692 ± 2	biotite granodiorite	Isaiah Creek stock	Group I transitional	scattered points about line drawn through 3 points to give max age of 2691.8 ± 2.2; LI = 670 ± 38 Ma; MSWD = 0.0.	Isaiah Creek stock
31	z3429	93HNB-9a2	<2689 ± 1	aphanitic felsic dyke	Kenogaming felsic dyke	Group I transitional	1 points, conc.; 2688.8 ± 1.0; also 2690.7 ± 1.1.	Hanrahan antiform
32	z4322	94HNB-286	2686 ± 1	hornblende diorite	Muskego diorite	Syntectonic	3 points conc. 2685.5 ± 0.6; MSWD = 0.74; POF = 48%; one 1.2 % disc.	Nat River granitoid complex
33	z3918	94HNB-1135a2	<2686 ± 1	biotite granodiorite	Smuts Pluton	Syntectonic	2 points through zero 2686.3 ± 0.7 max age; 5 points, conc to 1 % disc 2689 ± 1 Ma to 2716 ± 2 Ma.	Ramsey-Algoma granitoid complex
34			2684 ± 3	biotite granite	Hoodoo Lake Pluton	Syntectonic	U-Pb TIMS on zircon (Frarey and Krogh, 1986)	Hoodoo Lake Pluton (Northern Swayze)
35	z3023	92HNB-123a	2682 +3/-2	hornblende granodiorite	Neville Pluton	Syntectonic	2 points conc and 0.5 % disc; UI = 2681.8 +2.3/-1.4; LI = 0.82 ± 0.51 Ga; 1 point 0.1 % disc 2685 ± 2 Ma.	Kenogamissi granitoid complex
36	z4321	94HNB-283	2684 ± 2	hornblende monzonite	Kukatush Pluton	Syntectonic	3 points conc. to 0.4% disc; UI = 2684.2 ± 1.3; MSWD = 0.33; POF = 56%; forced through 1000 Ma.	Kukatush Pluton
37	z3024	92HNB-125a	2682 ± 1	hornblende granodiorite	Hillary Pluton	Syntectonic	4 points, 0.5 to 1.5 % disc; UI = 2681.6 ± 0.9, LI = 0.37 ± 0.5 Ga; MSWD = 1.4, POF = 25 %; single conc analysis at 2691 ± 2 Ma	Kenogamissi granitoid complex
38			2680 ± 3	hornblende diorite	Ivanhoe Lake Pluton	Syntectonic	U-Pb TIMS on zircon Percival and Krogh, 1983).	Ivan Lake Pluton (Northern Swayze)
39	z3917	94HNB-280	2674 ± 1	hornblende quartz diorite	Joffre Pluton	Group II transitional	4 points, 0.4 % to 1.1 % disc; UI = 2673.7 ± 0.7; LI = 392 ± 14 Ma; MSWD = 0.92; POF = 43%.	Ramsey-Algoma granitoid complex
40	z3935	94HNB-1286	2668 ± 1	hornblende monzonite	Margaret stock	Group II transitional	7 points, conc. to 0.7 % disc; UI = 2667.5 +0.9/-07; LI = 0.47 ± 0.40 Ga; MSWD = 0.76; POF = 58 %.	Ramsey-Algoma granitoid complex
41	z2835	92HNB-26b	2676 ± 4	biotite granite	Somme Pluton	Post-tectonic	U-Pb SHRIMP on zircon (O. van Breemen, unpub. SHRIMP U-Pb data).	Kenogamissi granitoid complex
42	z4191	95HNB-280	<2673 ± 2	biotite granite to granodiorite	Biggs Pluton	Post-tectonic	3 points 4.6 % to 8.9 % disc.; UI = 2673.3 ± 1.7; LI forced through origin; MSWD = 2.73, POF = 9.8%.	Biggs Pluton
43	z4320	92HNB-132f	2662 ± 4	biotite granite	Bardney Batholith	Post-tectonic	U-Pb SHRIMP on zircon (O. van Breemen, unpub. SHRIMP U-Pb data).	Ramsey-Algoma granitoid complex

MSWD = mean square of weighted deviates; POF = probability of fit; UI (LI) = upper (lower) intercept age calculated from discordia regression line; conc. = concordant; disc. = discordant

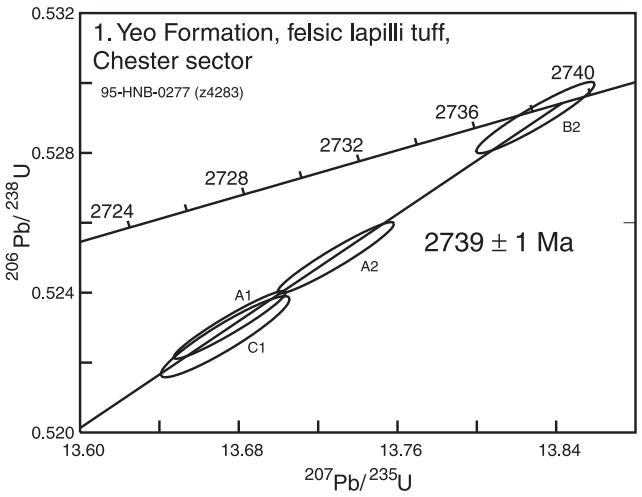

Figure 5. U-Pb concordia diagrams for zircon analyses from the Yeo Formation of the Chester Group.

No sample was obtained from the Chester Group in the type stratigraphic section, but a crosscutting felsic porphyritic dyke, the Strata Lake porphyry (sample 2, Fig. 4) provides an age of 2731 +7/-5 Ma based on an upper intercept of a regression line through five analyses (Fig. 6). Two slightly discordant analyses (A and D) yielded $^{207}Pb/^{206}Pb$ ages of ca. 2734 Ma and 2746 Ma, indicating a component of inherited radiogenic Pb. Some scatter in the remaining five analyses (MSWD = 5.7, Table 2) may also be due to inheritance. The age for this porphyry, which is a likely feeder to the Strata Lake Formation in the overlying Marion Group, is nevertheless interpreted as a minimum for the Yeo Formation. Samples of the tonalite intruding the Chester Group from the southwestern lobe of the Kenogamassi granitoid complex collected subsequent to this project yielded crystallization ages of 2747.3 ± 2.6 Ma and 2743.6 ± 1 Ma, further confirming the Pacaud assemblage age for this part of the stratigraphic column (O. van Breemen, unpub. SHRIMP U-Pb data). This assemblage has both ensimatic ocean basin and arc volcanic signatures in a tectonic environment interpreted to have mixed plume and subduction magmatic components (Ayer et al., 2002).

Marion Group

Overlying the Chester Group is the Marion Group, which is composed of three formations: 1) the mafic to intermediate volcanic rocks of the Rush River Formation, overlain by 2) felsic to intermediate volcanic rocks of the Strata Lake Formation, and capped by 3) the oxide-facies ironstones of the Woman River Formation. The Strata Lake Formation consists of massive, calc-alkaline felsic to intermediate flows, as well as ash and crystal tuffs interbedded with lapilli tuff and volcanic breccia. The upper portion of this formation is dominated by variably chloritized and sulphidized volcanic rocks related to crackle breccia zones that are interpreted to represent paleo-hydrothermal conduits for iron-rich fluids that precipitated out the overlying ironstones. The Marion Group was correlated with the 2730 to 2724 Ma Deloro assemblage of the southern Abitibi belt characterized by oceanic arc volcanic signatures interpreted to be associated with a subduction tectonic environment (Ayer et al., 2002).

The Strata Lake Formation is the only formation in which datable felsic volcanic rocks are found. Six ages were obtained, from south to north across the entire Swayze belt. A quartz-eye-bearing felsic volcanic breccia (sample 3) from this formation within the central Swayze type section yielded an age of 2735 +6/-4 Ma based on an upper intercept of a four point regression line (Fig. 6). Two concordant fractions, which are interpreted to be inherited, yielded $^{207}Pb/^{206}Pb$ ages of 2754 ± 2 Ma and 2752 ± 2 Ma. Discordant fractions B and E are also excluded from the age-regression analysis because of likely inheritance, while F is excluded because it appears to have suffered a more complex Pb loss history. An identical age of 2734 ± 2 Ma was obtained from equidimensional to stubby zircons from a felsic lapilli tuff (sample 4) from the Strata Lake Formation in the southeastern Chester sector (Fig. 2, 3). This age is based on the upper intercept of a regression line through 3 points; two of which are 0.2% and 0.8% discordant (D and A, respectively, Fig. 6) and a third is 9.6% discordant (Table 1, not plotted). Three analyses that are 0.5% to 1.2% discordant yield older $^{207}Pb/^{206}Pb$ ages of ca. 2741 Ma to 2737 Ma and are interpreted to contain inherited Pb components.

In the Shunsby sector, in the western Swayze belt (Fig. 3), there are two distinct units of banded iron-formation (BIF) that are stratigraphically equivalent to the Woman River Formation, each underlain by intermediate volcanic rocks. A felsic lapilli tuff in the Strata Lake Formation (sample 5) underlying the older BIF yields an age of 2731 ± 2 Ma based on a weighted average of the $^{207}Pb/^{206}Pb$ ages of two concordant and one 0.5% discordant point. Fifteen kilometres further west, a felsic crystal tuff (sample 6, Fig. 6) also underlying the older BIF yields an identical age of 2730 +3/-2 Ma based on a regression line through two concordant and one 0.4% discordant point (Fig. 6). A felsic volcanoclastic rock underlying the younger BIF (sample 7) yields an age of 2724 ± 1 Ma based on a regression line through two concordant and one 0.5% discordant analyses (Fig. 6). These data suggest that the two BIF bodies were deposited approximately 6 Ma apart. Iron-formation also occurs at different stratigraphic levels within the Deloro assemblage within the Shaw Dome in the Abitibi belt south of Timmins, where U-Pb TIMS analysis of zircons from felsic tuff intercalated with iron-formation in the upper part of the assemblage yielded an age of 2724.1 ± 3.7 Ma (Ayer et al., 2005). This upper iron-formation age correlates with the upper iron-formation in the Shunsby sector.

A feldspar-quartz porphyry (sample 8) was collected from Esther Township (Fig. 4) and is believed to be coeval with the overlying felsic volcanic rocks of the Marion Group. A regression line through three points that are concordant to

1.8% discordant yields an upper intercept age of 2724 +4/-3 Ma (Fig. 6). The large MSWD of 5.6 is attributed to slightly different Pb loss histories of the two discordant analyses and do not affect the upper intercept. The age is attributed to the time of emplacement and crystallization of a feeder dyke to the felsic volcanic rocks of the Marion Group.

In the northern section through the Hanrahan antiform (Fig. 3), a felsic lapilli tuff of the Strata Lake Formation (sample 9) underlying banded iron-formation yielded an age of 2730 ± 1 Ma based on the weighted average $^{207}Pb/^{206}Pb$ age of two concordant analyses (Fig. 6). The MSWD of 3.4 may indicate a slight inherited component. As in the central type section, there is only one banded ironstone horizon in the northern section. The age data suggest that only the older of the two banded iron-formation bodies in the Shunsby Sector is found in the central and northern sectors.

Biscotasing Group

The Biscotasing Group includes rocks within the southern 'Biscotasing' arm of the Swayze belt and rocks of similar age have been identified in the northern Swayze belt (Fig. 2, 3). The Biscotasing Group contains mafic and felsic metavolcanic rocks, chert-magnetite iron-formation and clastic sedimentary rocks that are highly strained and metamorphosed to amphibolite facies. These varied rocks have been correlated by Ayer et al. (2002) with the 2719 to 2711 Ma Kidd-Munro assemblage that has both plume and island-arc volcanic signatures. On a regional scale, Ayer et al. (2002) recognized that the Stoughton-Roquemaure assemblage is locally present underlying the Kid Munro assemblage. This assemblage, not hitherto recognized in the Swayze belt, has a plume geochemical signature and its deposition was associated with an extensional tectonic environment.

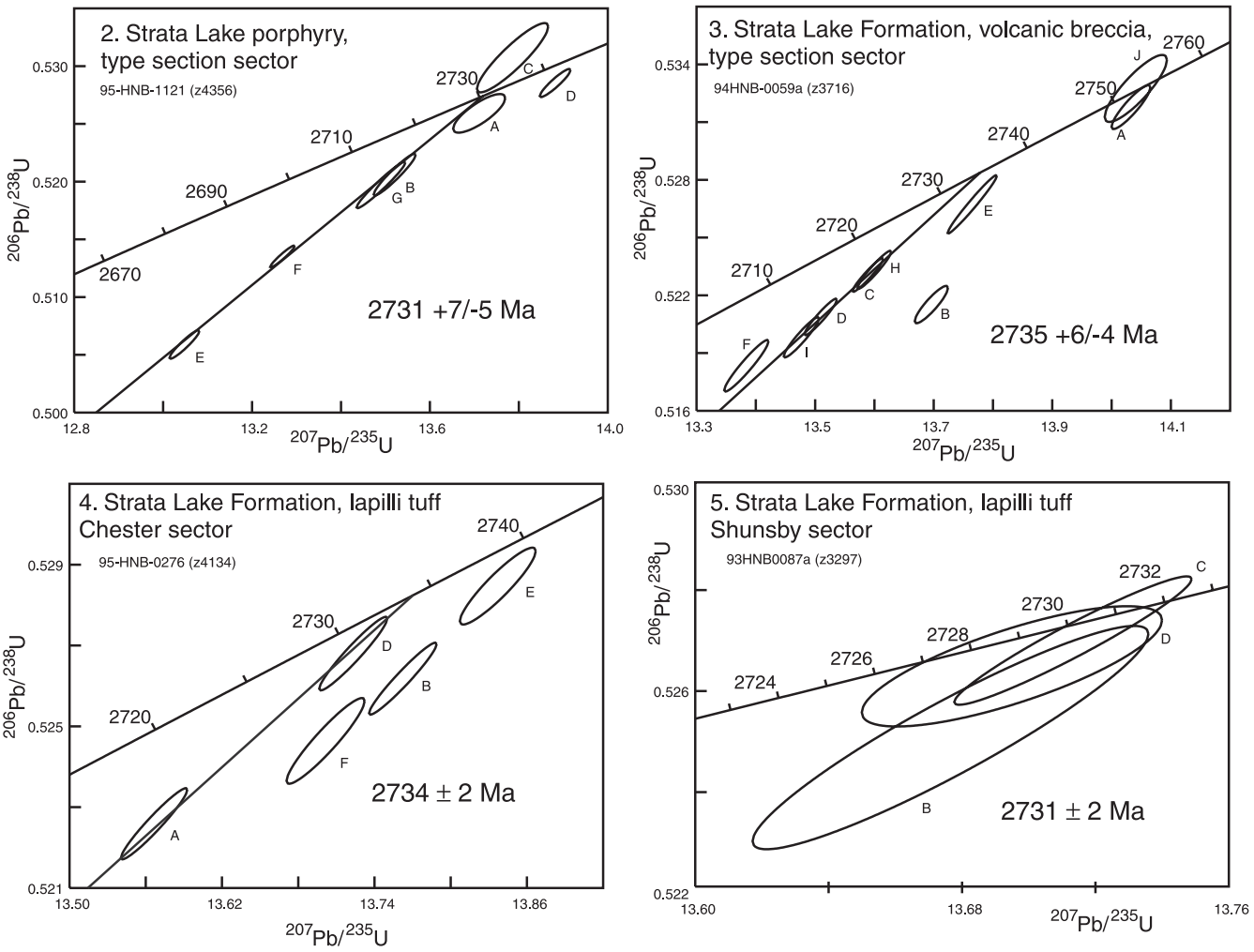

Figure 6. U-Pb concordia diagrams for zircon analyses from the Strata Lake Formation of the Marion Group and porphyry dykes interpreted as feeders to the Strata Lake Formation.

A quartz-phyric felsic flow (sample 10) from the Biscotasing group in the Swayze belt arm extending to the southeast of Ramsey (Fig. 3, 4) yields a U-Pb zircon upper intersection age of 2715 ± 2 Ma for a four-point regression line with points that are 0.3% to 1.0% discordant (Fig. 7). The Biscotasing Group does not outcrop in the central area, but two samples were collected from the northern Swayze belt (Fig. 3). A quartz-phyric felsic volcanic rock (sample 11) from the northern Swayze belt yields a 2718 ± 2 Ma upper intercept age for a regression line through three points, two concordant and one 1.2% discordant (Fig. 7). Another sample from the northern Swayze, a felsic flow breccia (sample 12) yields a weighted average $^{207}Pb/^{206}Pb$ age of 2715 ± 2 Ma of four points that are concordant to 0.3% discordant (Fig. 7). Two points are strongly discordant. These ages confirm the north-to-south correlation of units across a gap in the central Swayze belt. A stratigraphic gap, thought to represent a submarine unconformity, exists between the Deloro and Tisdale assemblages in the central part of the Abitibi belt between the Porcupine-Destor and Larder Lake-Cadillac deformation zones (Ayer et al., 2002; Ayer et al., 2005).

Trailbreaker Group

Directly overlying the Marion Group in the central Swayze belt is the Trailbreaker Group, which includes mafic to intermediate volcanic rocks of the October Lake Formation and felsic to intermediate volcanic rocks of the overlying Heenan Formation. The Heenan Formation has not been identified in the northern Swayze belt. The Trailbreaker Group has been correlated by Ayer et al. (2002) with the 2710 to 2704 Ma Tisdale assemblage of the Abitibi belt that has both plume and island-arc volcanic chemical signatures.

One direct stratigraphic age was obtained from the Heenan Formation, in the type section sector (Fig. 3). A felsic volcanic rock (sample 13) yields a U-Pb zircon upper intercept age of 2705 ± 2 Ma for a regression line through 4 points that are concordant to 3.4% discordant (Fig. 8). One concordant and one 0.7% discordant analyses yield older $^{207}Pb/^{206}Pb$ ages of 2731 ± 3 Ma and ca. 2740 Ma and are interpreted to be inherited. In the same section a quartz-feldspar porphyry body (sample 14) intrudes the underlying Strata Lake Formation of the Marion Group. Four zircon analyses

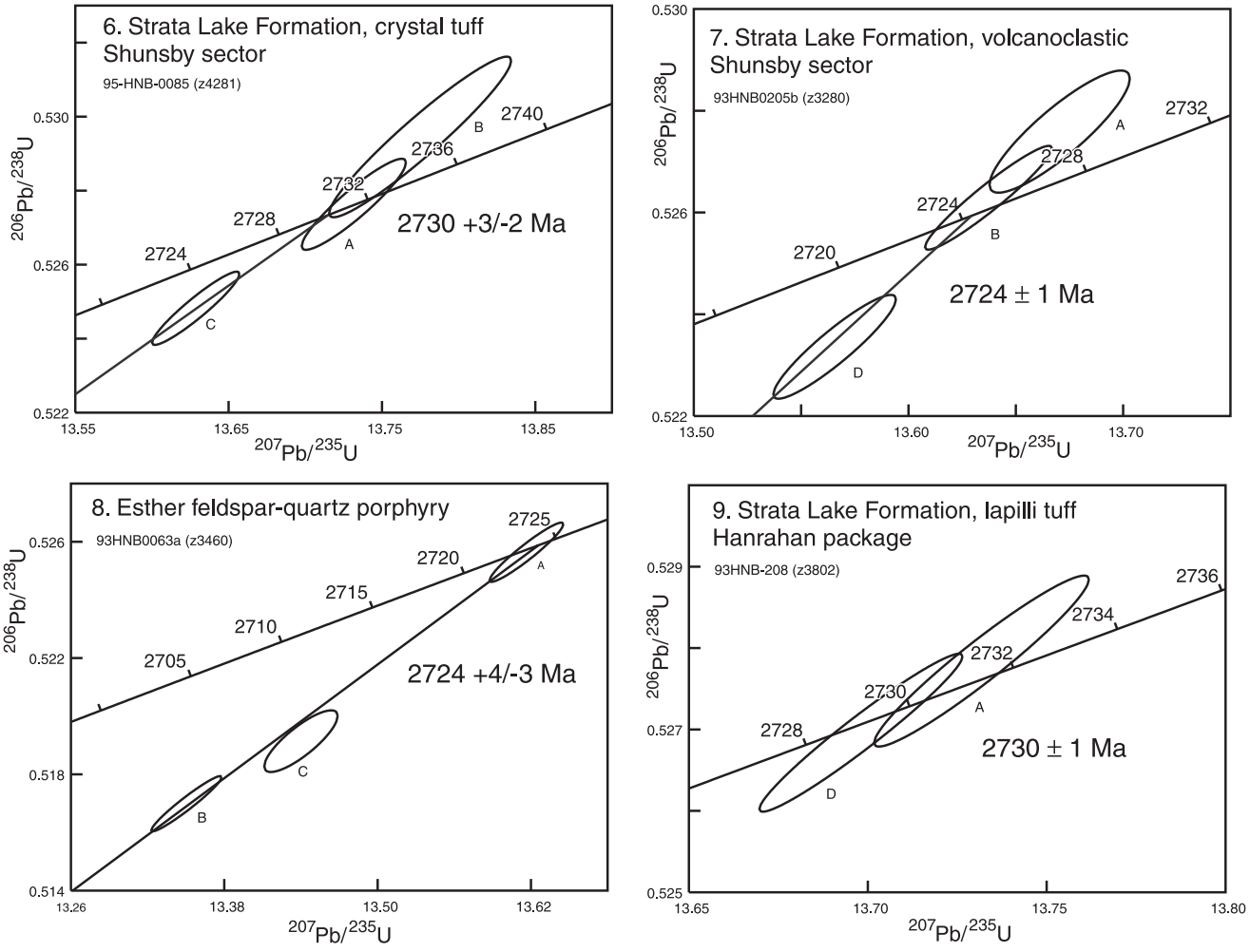

Figure 6 (cont.)

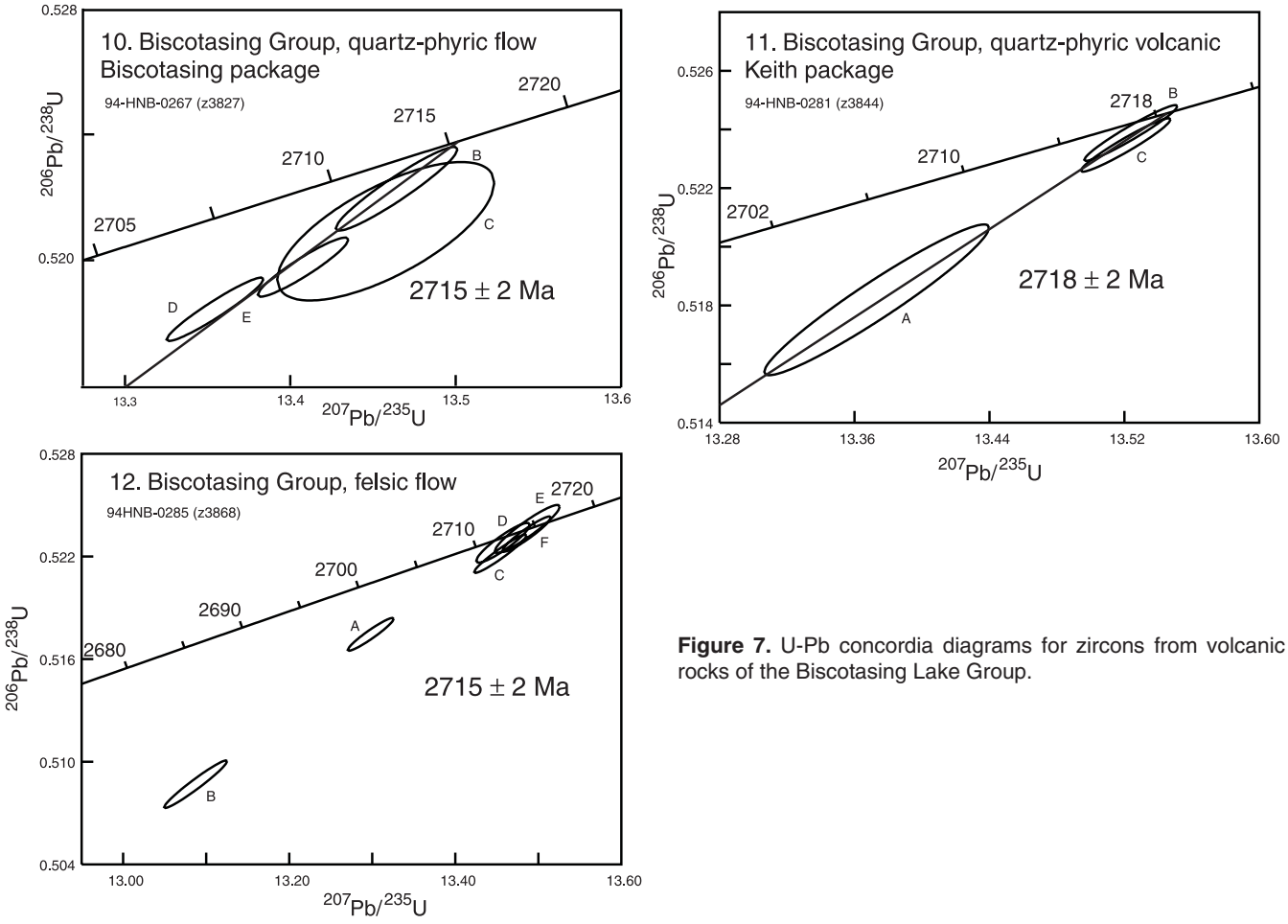

Figure 7. U-Pb concordia diagrams for zircons from volcanic rocks of the Biscotasing Lake Group.

that are concordant to 0.9% discordant yield a weighted mean $^{207}Pb/^{206}Pb$ age of 2705 ± 2 Ma (Fig. 8). The slightly younger age for fraction E is attributed to Pb loss during the late Archean or early Proterozoic. The age suggests that this intrusion is a feeder to the Heenan Formation. Two 1.5% and 1.7% discordant analyses have $^{207}Pb/^{206}Pb$ ages of ca. 2739 Ma and 2722 Ma that are interpreted to reflect an inherited component. Along the north-central section, a felsic volcanoclastic rock (sample 15) yields four overlapping to slightly discordant U-Pb zircon analyses. A weighted average of their $^{207}Pb/^{206}Pb$ ages yields 2702 ± 1 Ma.

Swayze Group

Overlying the Trailbreaker Group is the Swayze Group, which includes the Newton, Brett Lake, and Denyes formations. The Newton Formation consists of an extensive package of mafic and ultramafic volcanic flows and sills, whereas the overlying Brett Lake Formation consists of felsic to intermediate volcanic, volcaniclastic and clastic rocks. These volcanic strata are in turn conformably to disconformably overlain by the clastic sedimentary rocks of the Denyes Formation. The Swayze Group is correlated with the 2703 to 2696 Ma Blake River assemblage of the central east and northeastern parts of the Abitibi belt (Ayer et al., 2002; Ayer et al., 2005).

The Brett Lake Formation was first dated at 2697 ± 1 Ma (sample 17, Table 2, Fig. 3) in the type section sector by Cattell et al. (1984). In this study it was possible to date felsic volcanic rocks of the Brett Lake Formation in both the north-central and Shunsby sectors. Multi-faceted yellow-brown zircons from a felsic ash from the type section (sample 18) yielded six concordant to 0.4% discordant analyses. A weighted average age of their $^{207}Pb/^{206}Pb$ ages is 2695 ± 2 Ma (Fig. 9). A felsic crystal tuff from the Shunsby sector (sample 19) yielded an upper intercept age of 2695 ± 2 Ma for a regression line through five points that are concordant to 1.5% discordant.

A quartz-feldspar porphyry (QFP) dyke in the Shunsby area appears to be axial planar to F_2 folds (that fold an S_1 foliation) and was collected (sample 16) with a view to providing a minimum age of F_2 folding in the area. U-Pb analyses yield an age of 2699 +3/-2 Ma based on a regression line through three points that are 0.5% to 1.8% discordant (Fig. 9). This age is too old to be associated with the F_2 deformation and the intrusion is interpreted to be a feeder to volcanic rocks in the Swayze Group.

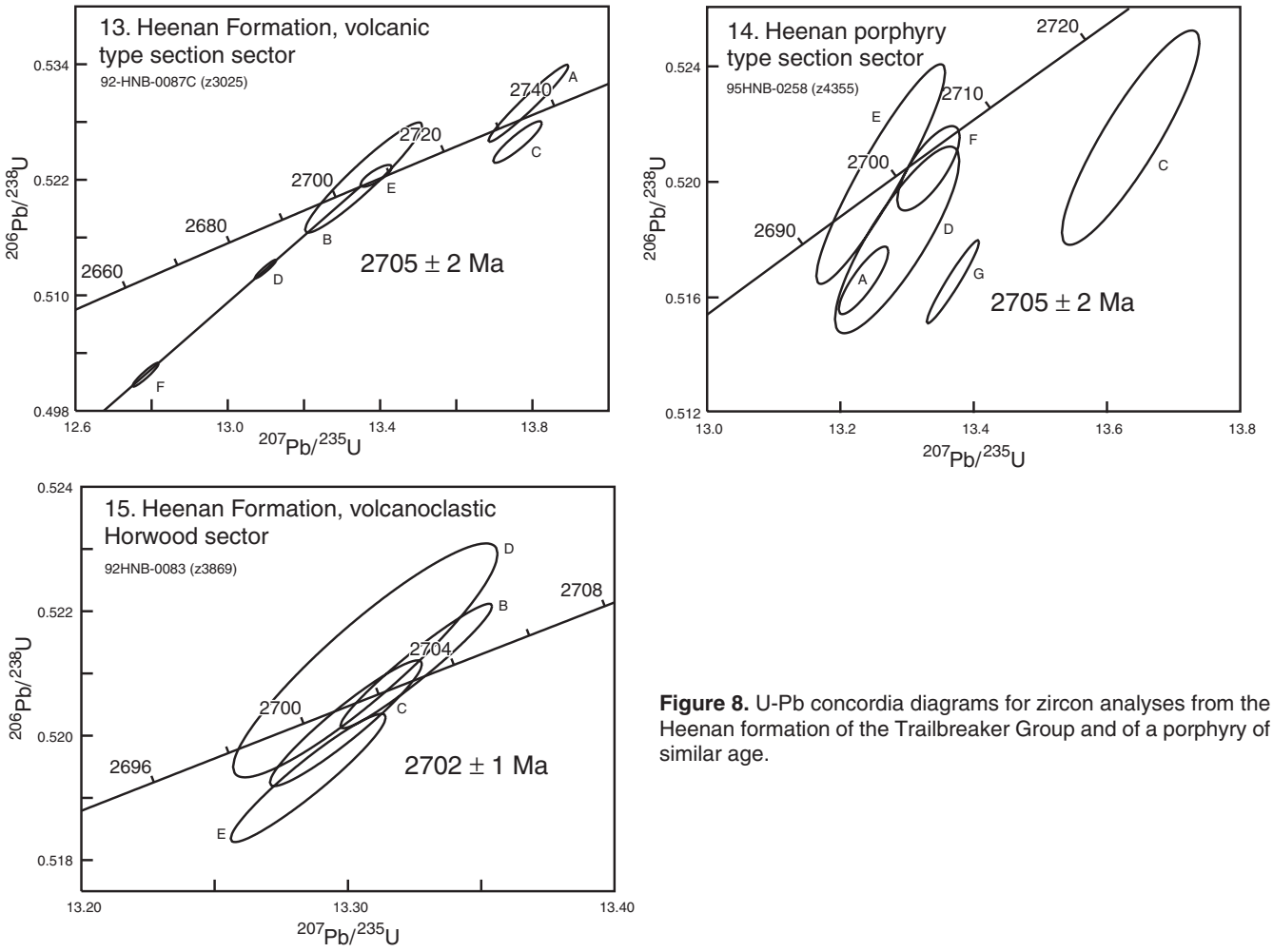

Figure 8. U-Pb concordia diagrams for zircon analyses from the Heenan formation of the Trailbreaker Group and of a porphyry of similar age.

Single zircons were analyzed for two sandstone samples from the Denyes Formation. Some crystals are rounded, while others show sharp facets. From the western Swayze greenstone belt (Fig. 3, 4), the 'Raney River' sandstone (sample 20) yielded a narrow spread of dates mostly equivalent to the underlying volcanic rocks, i.e. seven ages fall between 2724 Ma and 2695 Ma. An upper age limit for deposition of 2683 ± 6 Ma (Fig. 9) is assigned from concordant analysis B3. Sharply faceted zircons from a sandstone (sample 21) of the Denyes Formation along the northern section yield a similar tight cluster of 10 dates between 2716 Ma and 2695 Ma, equivalent to ages of local volcanic rocks. A maximum depositional age of 2695 ± 1 Ma is established from concordant analysis H.

Ridout Group

All of the aforementioned groups and formations are overlain by the younger sedimentary and volcanic rocks of the Ridout Group, which includes the Opeepeesway Formation and the North Arm Formation. The Ridout Group forms long linear units that are spatially associated with regional D_2 and D_3 high-strain zones that transect the belt in an east-west orientation. These high-strain zones bound the northern and southern margins of the Kenogamissi Batholith and continue into the Abitibi greenstone belt (Fig. 2). The Ridout Group can be correlated across the southern Abitibi belt with the 2676 to 2670 Ma Timiskaming assemblage that has been associated with a continental arc (Ayer et al., 2002; Ayer et al., 2005).

A sample of the Opeepeesway Formation (sample 22) was collected from near the type locality near Opeepeesway Lake (Fig. 4) and contained prismatic zircon showing no evidence of rounding. Eight zircons yielded dates from 2742 Ma to 2737 Ma and only two yielded younger dates (Fig. 10). Thus, unlike the sandstone from the Denyes Formation, detrital zircons were not derived from immediately underlying volcanic rocks, but from the lower part of the Swayze belt succession. A maximum age of deposition of 2688 ± 2 Ma is based on the 0.5% discordant analysis K (Table 1).

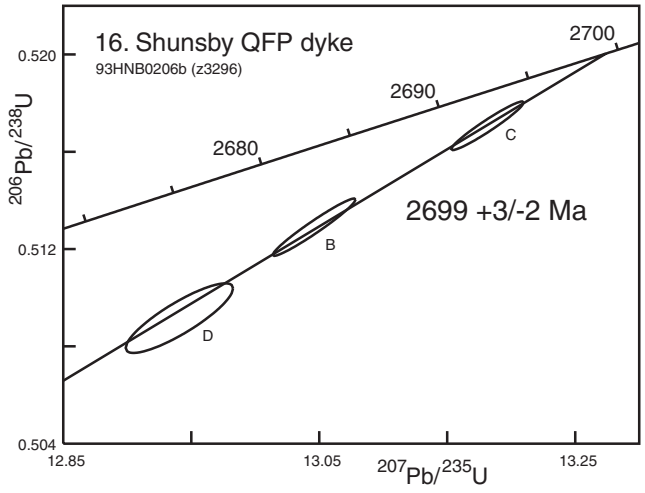

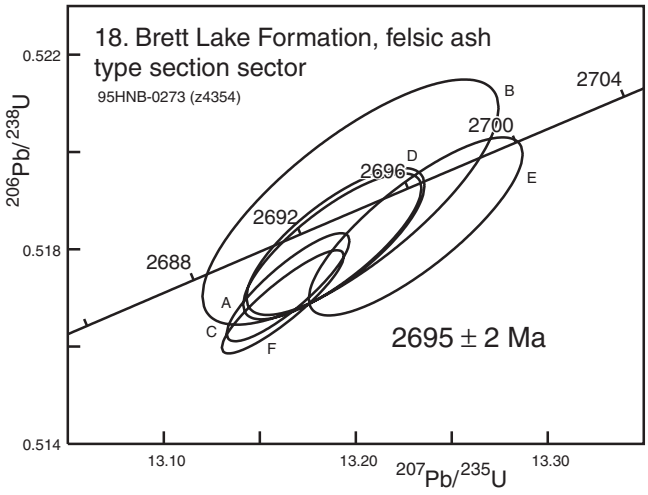

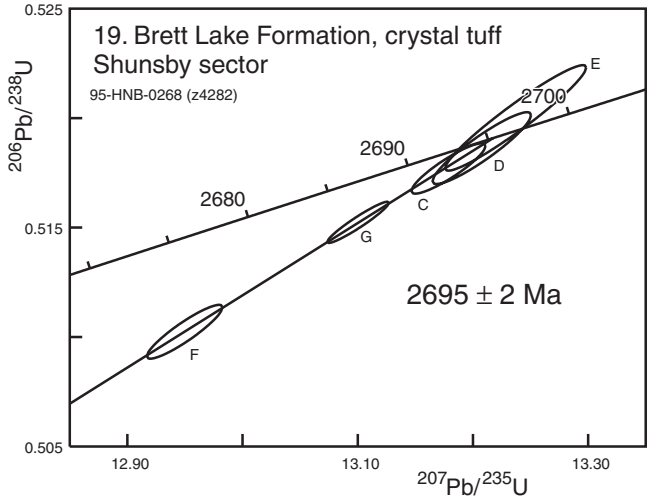

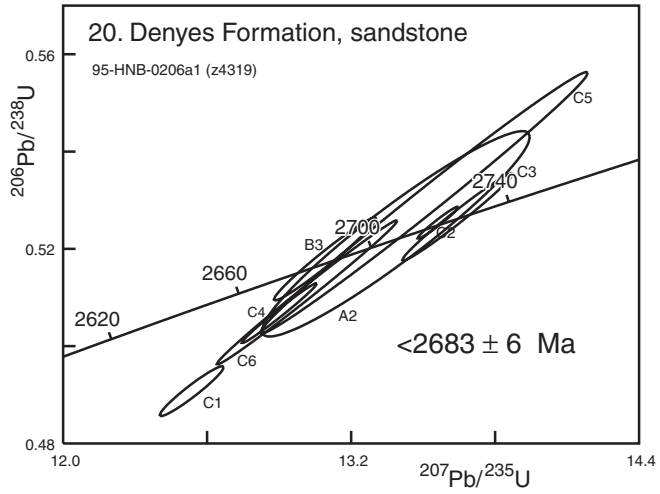

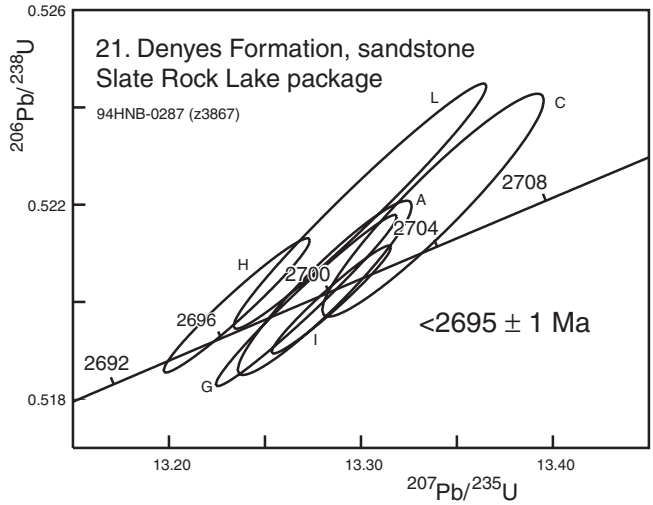

Figure 9. U-Pb concordia diagrams for multigrain zircon analyses from volcanic rocks of the Brett Lake Formation and single grain zircon analyses from clastic sediments of Denyes Formation of the Swayze Group.

SUBDIVISION OF GRANITIC ROCKS

The Swayze greenstone belt is bordered to the north, east, and south by large granitoid complexes (Fig. 2). The poorly exposed Nat River granitoid complex underlies the area just north of the study area. The elliptical Kenogamissi granitoid complex separates the Swayze belt from the Abitibi belt. The Ramsey-Algoma granitoid complex extends southward to the Sudbury structure and comprises one of the largest areas of continuous granitoid rocks in the southern Superior Province.

The felsic to intermediate granitoid rocks were subdivided by Heather (1998, 2001) into five broad categories based on the results of mapping and geochronology:

- Synvolcanic diorite, biotite and hornblende tonalite (trondhjemite) and granodiorite intrusions ranging in age from 2740 Ma to 2696 Ma. Synvolcanic batholiths are dominantly sheet-like and are folded, along with supracrustal rocks, into antiformal culminations.

- A transitional suite ranging in age from 2695 Ma to 2686 Ma, and comprising tonalite to quartz monzonite intrusions.

- Syntectonic hornblende granodiorite intrusions ranging in age from 2685 Ma to 2680 Ma. They occur as both large sheet-like intrusions localized along the contact between greenstone belt rocks and the synvolcanic intrusions, and as discrete plutons and stocks within both the greenstone belt and synvolcanic intrusive bodies. At the regional scale they tend to follow F_2 anticlinal axes but also occur locally along F_2 synclinal axes.

- A second transitional suite including diorite to monzonite intrusions ranging in age from 2680 Ma to 2665 Ma.

- Non-foliated, ca. 2665 Ma, post-tectonic granite intrusions occurring as large batholiths and dyke swarms within areas of synvolcanic and syntectonic intrusions, generally away from the greenstone belt. They feature local igneous layering and appear to have been passively emplaced.

GEOCHRONOLOGY OF PLUTONIC ROCKS

This study presents the results of 19 felsic to intermediate plutonic rocks in the chronological order of the above categories. Sample locations are given in Figure 11. For more complete geological details, the reader is referred to Heather 1998 and 2001. U-Pb analytical results are given in Table 3 and

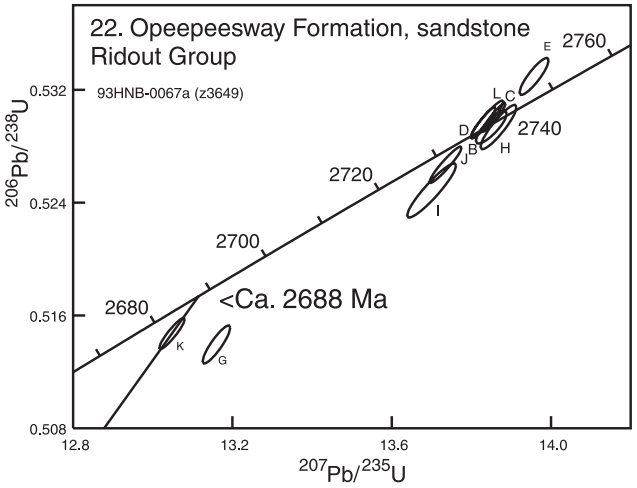

Figure 10. U-Pb concordia diagram for single zircon analyses from a clastic sediment of the Opeepeesway Formation of the Ridout Group.

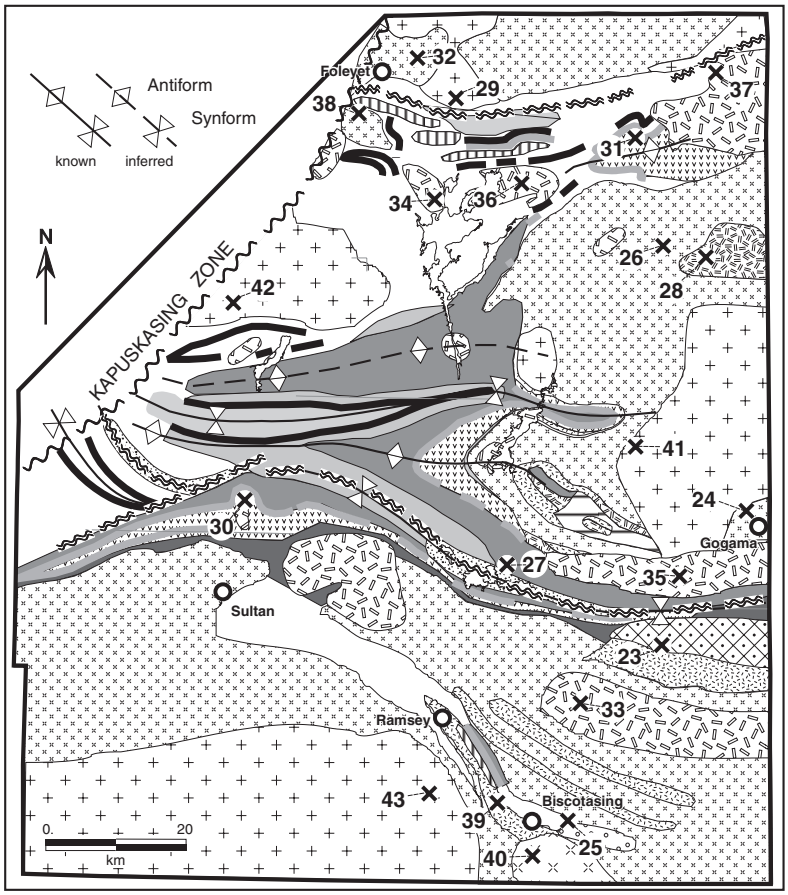

Figure 11. Map of the Swayze greenstone belt showing geochronology sample locations for plutonic rocks. Legend the same as Figure 2.

displayed in concordia diagrams (Fig. 12–16). Table 4 provides a summary of ages, age interpretation, as well as nomenclature. Although Heather and Shore (1999) quote an age of 2727 +11/-9 Ma for the Arbutus tonalite of the Ramsey-Algoma Granitoid Complex, this estimate is based on three highly discordant analyses, considered unreliable and is not included in this report.

Synvolcanic intrusions

Synvolcanic intrusions are typically sheet-like in geometry (i.e. laccolithic) and vary from massive, nonfoliated to strongly foliated through locally gneissic in texture. Magma-mixing textures and igneous layering are common. Where synvolcanic units are in contact with greenstone belt rocks, metamorphic grade is amphibolite facies. Generally, adjacent to these contacts, both the intrusive and supracrustal rocks are highly strained. Synvolcanic units dated in this study include the Chester granitoid complex (sample 23), the Gogama tonalite (sample 24), the Biscotasing tonalite (sample 25), the Regan tonalite (sample 26), and the Heenan porphyry (sample 27). It is not always possible to distinguish with confidence between a synvolcanic intrusion and a feeder dyke, which is the case for the Heenan porphyry.

The oldest age obtained from the Swayze belt in the course of this study was from the biotite trondhjemite of the Chester granitoid complex, emplaced along the Ridout syncline in the southeastern arm of the Swayze belt, where it disrupts strata of the Chester Group. This complex, a crudely stratified trondhjemite-diorite laccolith, contains numerous screens and inclusions of mafic volcanic rocks. A leucocratic, quartz-rich biotite trondhjemite (sample 23) was sampled. On a concordia plot (Fig. 12), 4 analyses are collinear and are concordant to 1.0% discordant. Linear regression yields an upper intercept age of 2740 ± 2 Ma, which is within error of the 2739 ± 2 Ma age of the Yeo Formation (Table 2). Tonalite samples from the southwestern lobe of the Kenogamassi granitoid complex collected subsequent to this project yielded crystallization ages of 2747.3 ± 2.6 Ma and 2743.6 ±1 Ma respectively (O. van Breemen, unpub. SHRIMP U-Pb data).

An orthogneiss (sample 24) was collected just north of the town of Gogama (Fig. 11). This outcrop of rare gneissic-textured tonalite has the appearance of an older prevolcanic igneous phase. One concordant and one 0.3% discordant analyses yield a weighted average $^{207}Pb/^{206}Pb$ age of 2722 ± 1 Ma (Fig. 12). Two fractions have ages of ca. 2734 Ma and 2728 Ma and are interpreted to be inherited. There is, however, no indication that this unit constitutes prevolcanic basement to the Swayze belt. The orthogneiss is, therefore, interpreted as a synvolcanic intrusion that experienced partial melting during peak metamorphism and deformation at mid-crustal levels.

The Biscotasing tonalite (sample 25) is a distinctive unit of foliated, quartz-porphyritic biotite granodiorite to tonalite that extends from the town of Biscotasing as far south as the Margaret stock (Fig. 2, 11). Along its western margin, this unit appears to be transitional into high-level, mafic to felsic intrusive sills and volcanic flows of the Biscotasing arm greenstone belt, suggesting that they are cogenetic. A regression line through four, 0.4% to 1.0% discordant, zircon analyses (Fig. 12) yields an upper intercept age of 2715 +3/-2 Ma, which is interpreted as the time of granodiorite emplacement and crystallization.

The Regan hornblende tonalite (sample 26) was sampled from the north-central area of the Kenogamissi Batholith. A cluster of mostly concordant analyses is aligned with the exception of analysis A, which may have experienced slightly different Pb loss. Regression of the remaining 5 data points yields an upper intercept age of 2715 ± 2 Ma, which is interpreted as the time of igneous emplacement and crystallization (Fig. 12). The Northrup tonalite (sample 28) also from the Kenogamissi Batholith, yields a crystallization age of 2698 ± 1 Ma based on the weighted average of $^{207}Pb/^{206}Pb$ ages that are 0.3% -0.6% discordant (Fig. 12). In the Chester sector, a quartz-feldspar intrusion, the Heenan porphyry (sample 27), yielded two concordant analyses with a weighted average $^{207}Pb/^{206}Pb$ age of 2707 ± 1 Ma. This unit may have been a feeder to the overlying felsic volcanic rocks of the Heenan Formation.

Group I transitional intrusions

Several intrusions have been mapped and dated that share characteristics of both the synvolcanic group and the syntectonic group and these include the Nat River granodiorite pluton (sample 29) and the Isaiah Creek stock (sample 30). The Nat River, or Muskego, granodiorite pluton occurs within the Nat River granitoid complex in the northern Swayze belt. This pluton is poorly exposed and consists of massive to weakly foliated hornblende-biotite granodiorite tonalite and associated aplite dykes. A sample of biotite granodiorite (sample 29) yielded a scatter of data points ranging in $^{207}Pb/^{206}Pb$ age from 2705 ± 1 Ma to 2692 ± 2 Ma (Fig. 13). These data establish a maximum emplacement age of 2692 ± 2 Ma for the Nat River Granodiorite.

The Isaiah Creek stock (sample 30) consists of massive, nonfoliated, equigranular to locally potassium-feldspar-megacrystic, biotite granite to granodiorite. It is an elliptical intrusion, segmented by late northwest-striking faults. The stock displays good cumulate texture with plagioclase being more abundant than potassium feldspar. On a concordia diagram the data is both discordant and scattered. A regression line through points C (0.5% discordant), A, and F yields an upper intercept of 2692 ± 2 Ma, which is interpreted as a maximum age for the intrusion.

An aphanitic felsic dyke (sample 31), the Kenogaming felsic dyke, was collected from the immediate footwall rock to the Hanrahan Iron Formation. It is a massive, cleaved and fractured, feldspar-bearing rock with no apparent quartz. This sample was originally collected to provide an age for the upper part of the Hanrahan volcanic complex. The age of 2689 ± 1 Ma of the younger of two concordant analyses (Fig. 13) provides a maximum for the time of emplacement.

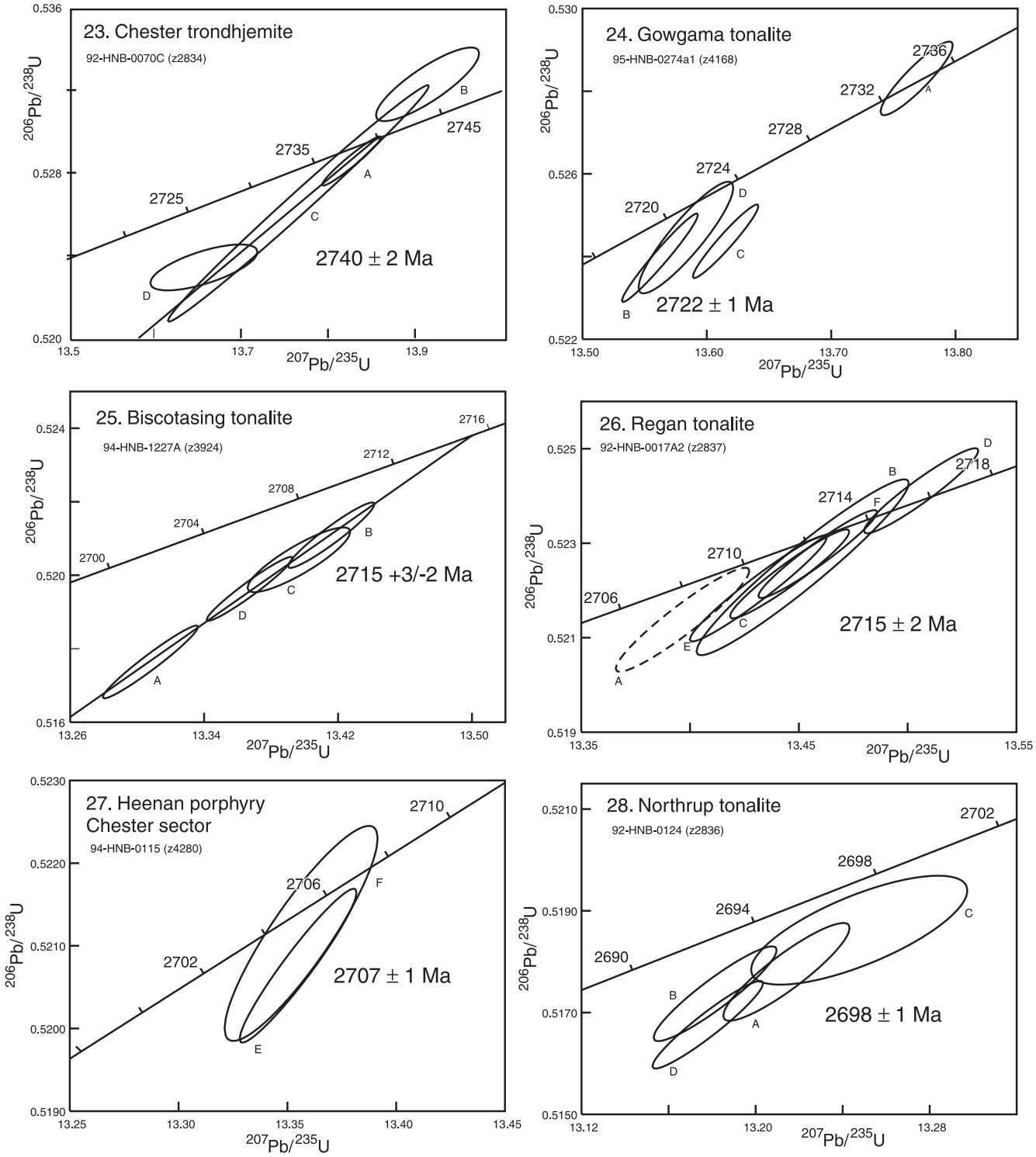

Figure 12. U-Pb concordia diagrams for zircon analyses from synvolcanic plutons: Chester trondhjemite, Gowgama tonalite, Biscotasing Lake pluton, Regan tonalite, Northrup tonalite, and Heenan porphyry.

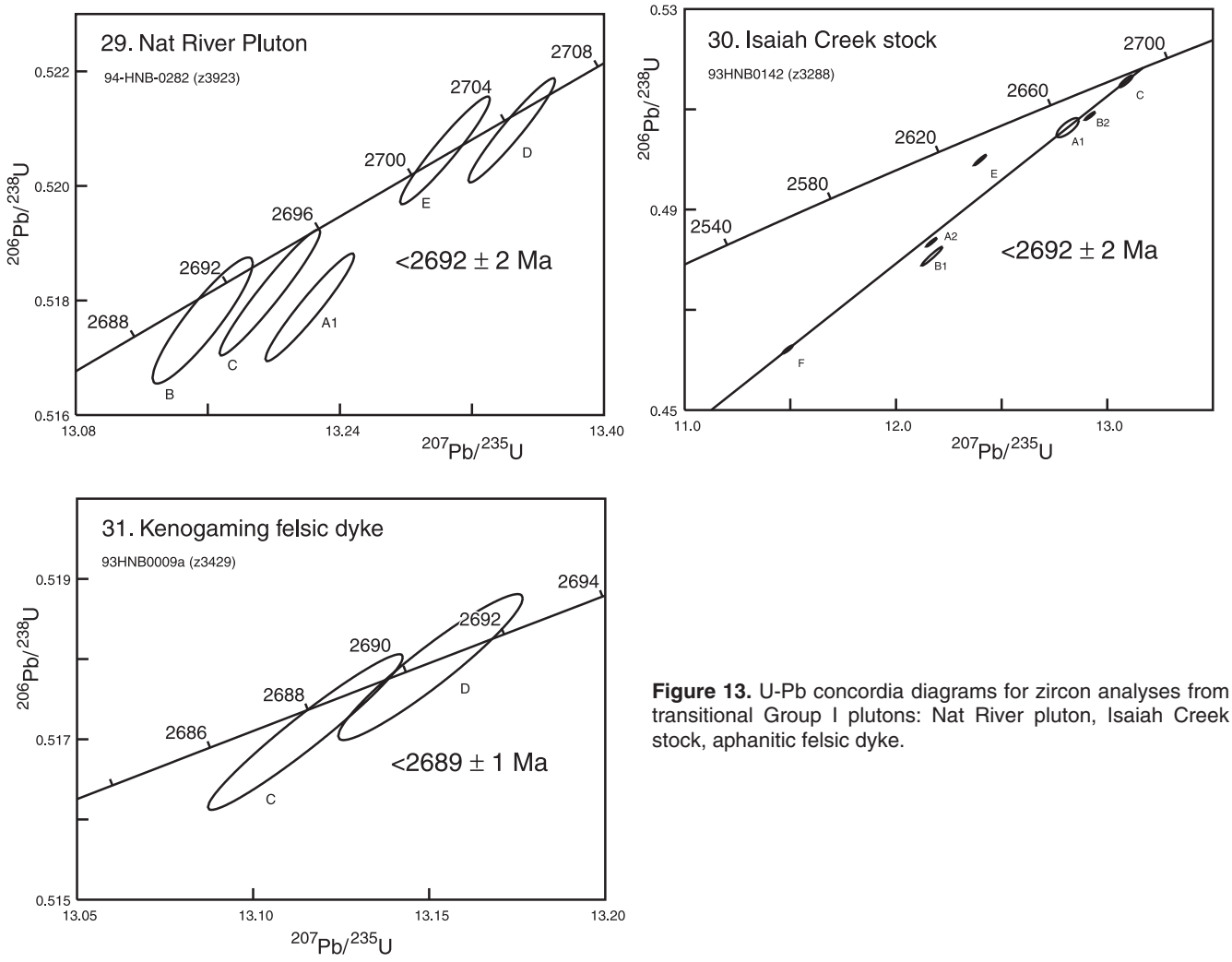

Figure 13. U-Pb concordia diagrams for zircon analyses from transitional Group I plutons: Nat River pluton, Isaiah Creek stock, aphanitic felsic dyke.

As the age is too young to be linked with Swayze belt volcanism, emplacement of the dyke is interpreted in terms of magmatism associated with the transitional plutonic phase.

Syntectonic intrusions

Granitoid intrusions that are syntectonic relative to the regional D_2 deformation form a distinctive suite based on their rock types, textures, and ages. These intrusions are distributed across the Swayze belt within broad corridors that flank the major east-west-trending Slate Rock and Ridout high-strain zones. They consist of massive to variably foliated, typically potassium-feldspar-megacrystic hornblende granodiorite, granite, monzonite, and quartz monzonite. Characteristic mafic cognate inclusions are common, as are magma-mixing and co-mingling textures. The Kukatush (sample 36), Hoodoo (sample 34), Muskego (sample 32), and Hillary (sample 37) plutons form a linear string of intrusions within the northern Swayze belt. Two syntectonic intrusions that were previously dated are the 2684 +3/-1 Ma Hoodoo Lake pluton (Frarey and Krogh, 1986) and the 2680 +3/-2 Ma Ivanhoe Lake pluton (Percival and Krogh, 1983); both are found along the northern margin of the Swayze belt.

The Muskego Pluton of dioritic composition is a major phase of the Nat River granitoid complex occurring along its southern margin (Fig. 11). Sample 32 was collected from massive to foliated, medium- to coarse-grained, hornblende diorite to quartz diorite containing hornblenditic enclaves. This sample contained equidimensional and anhedral brown zircons, from which three concordant to slightly discordant analyses yielded a weighted mean $^{207}Pb/^{206}Pb$ age of 2686 ± 1 Ma (Fig. 14).

The Smuts Pluton is a linear-shaped intrusion with an east-southeast orientation, parallel to the regional D_2 structural fabric located within the northern part of the Ramsey-Algoma granitoid complex. It consists of massive to weakly foliated, typically medium-grained, locally potassium-feldspar-megacrystic, biotite granodiorite to granite. Zircons from sample 33 yielded scattered concordant to 1.0 % discordant analyses with $^{207}Pb/^{206}Pb$ ages from ca. 2686 Ma to 2716 Ma (Fig. 14). The scatter in data points is

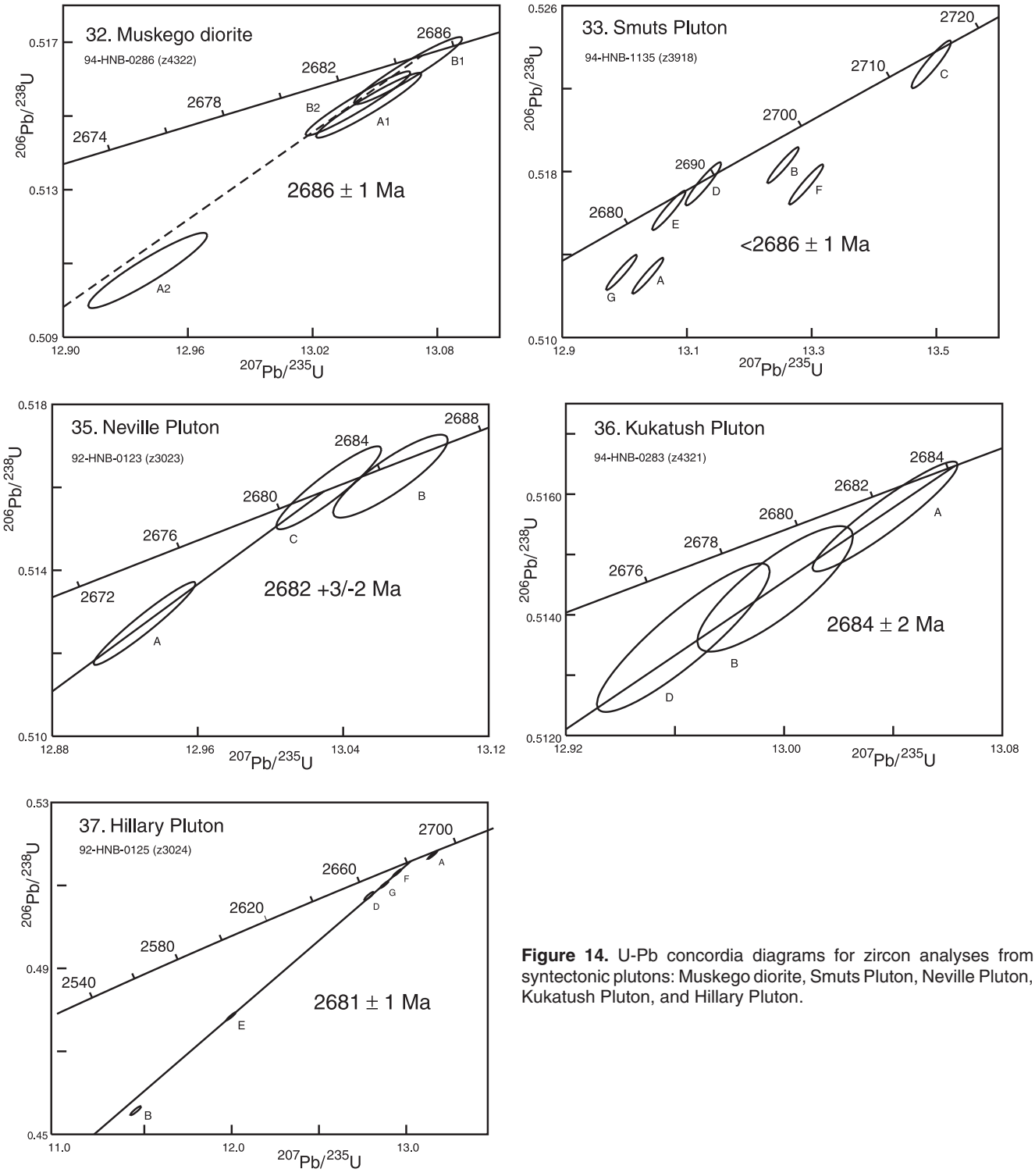

Figure 14. U-Pb concordia diagrams for zircon analyses from syntectonic plutons: Muskego diorite, Smuts Pluton, Neville Pluton, Kukatush Pluton, and Hillary Pluton.

attributed to inherited zircon. A line through points E and G cuts the concordia at 2686 ± 1 Ma and is interpreted as a maximum age for crystallization and emplacement of the Smuts Pluton.

The Neville Pluton is a crescent-shaped intrusion located along the southwestern margin of the Kenogamissi granitoid complex where it is localized along the contact between greenstone belt rocks to the south and synvolcanic tonalite to the north. It consists of massive to foliated, typically potassium-feldspar-megacrystic, hornblende granodiorite, granite, monzonite, and quartz monzonite. A foliated, hornblende, potassium-feldspar-megacrystic granodiorite (sample 35) yields an age of 2682 +3/-2 Ma based on two analyses, one concordant and one 0.5% discordant. A third, concordant fraction yielding a $^{207}Pb/^{206}Pb$ age of 2685 ± 2 Ma is interpreted as inherited.

The Kukatush Pluton, within the northern Swayze belt, consists of massive to foliated, medium-to coarse-grained, occasionally potassium-feldspar-megacrystic, hornblende and/or granodiorite, granite, and quartz monzonite. A sample of hornblende monzonite (sample 36) yielded an age of 2684 ± 2 Ma based on a discordia through one concordant analyses and two that are 0.3% and 0.4% discordant. The line is forced through 1.0 Ga, which is the lower intercept of a regression for the three data points.

The Hillary Pluton occurs in the northern Swayze belt along the axis of the Hanrahan anticline and between the Porcupine-Destor deformation zone and the Kenogamissi Batholith. It consists of massive to foliated, medium- to coarse-grained, occasionally potassium-feldspar-granodiorite to granite with mafic and hornblendite cognate inclusions. A foliated potassium-feldspar-megacrystic, hornblende granodiorite (sample 37) yields collinear analyses that are from 0.5% to 11.3% discordant. A line through the three least discordant points and analysis E yields an upper intercept age of 2681 ± 1 Ma (Fig. 14). It is assumed that the most discordant analysis, B, reflects inherited zircon as does concordant fraction A with a $^{207}Pb/^{206}Pb$ age of 2691 ± 2 Ma.

Group II transitional intrusions

Group II transitional intrusions make up a distinctive mappable group that shares characteristics with both the ca. 2680 Ma syntectonic group and the ca 2665 Ma post-tectonic group. Two intrusions of this group have been dated, the Joffre Pluton and the Margaret stock.

The Joffre Pluton is a distinctive sinuous, laccolith-shaped body, approximately 25 km long by 3 km wide, adjacent to the southern margin of the Biscotasing Arm of the Swayze belt. It consists of weakly to strongly foliated, leucocratic, medium- to coarse-grained, quartz monzodiorite, granodiorite, hornblende diorite, and quartz diorite. Zircons from a hornblende-quartz diorite (sample 39) include some elongate prismatic (fractions A to D) and some anhedral equidimensional (fractions E to G) (Fig. 15). An upper intercept age of 2674 ± 2 Ma is obtained from a regression through the four least discordant points A, D, F, and G.

The 100 km^2 Margaret stock, located at the eastern terminus of the Biscotasing Arm of the Swayze belt, consists of massive, pink- to red-weathering, coarse-grained, hornblende monzonite, quartz monzonite, and quartz syenite. Although the stock is typically coarse grained and equigranular, potassium feldspar megacrysts up to 3 cm in size are common. Zircons from a hornblende, potassium-feldspar-megacrystic monzonite (sample 40) yielded a linear regression upper intercept age of 2668 ± 1 Ma for 7 concordant to 0.7% discordant analyses.

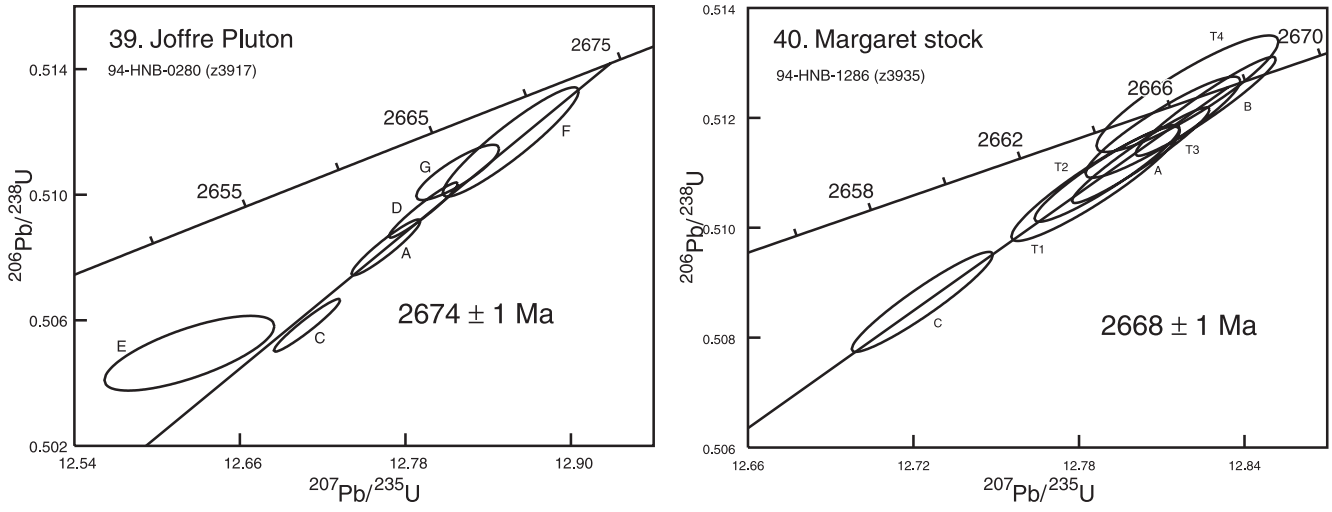

Figure 15. U-Pb concordia diagrams for zircon analyses from transitional II plutons: Joffre Pluton and Margaret stock.

Post-tectonic intrusions

A distinctive suite of granitoid intrusions are interpreted to be post-tectonic relative to the regional deformation on the basis of rock type, texture, and age. Although these intrusions are distributed across the Swayze belt, they are more abundant within the large Nat River, Kenogamissi and Ramsey-Algoma granitoid complexes. The group consists of unfoliated, massive, equigranular, biotite granite to granodiorite with associated pegmatite and aplite dykes. Three large intrusions of this type are the Somme Pluton in the east, the Biggs Pluton in the north, and the Bardney Lake Batholith in the south.

The Biggs Pluton, located in the northwestern part of the current map area, intrudes and metamorphoses mafic volcanic rocks of the Newton Formation on its southern, eastern, and northern contacts and is bounded to the west by the Kapuskasing Structural Zone. It consists of massive, pink-coloured, medium- to coarse-grained, biotite granite to granodiorite with local pegmatitic phases and occasional cognate inclusions of hornblende diorite to quartz diorite. A biotite granite-granodiorite (sample 42) has four discordant analyses of which three are collinear. A regression line through these and the origin yields an upper intercept age of 2673 ± 2 Ma (Figure 16). This age needs to be taken with caution in view of the strong discordance and the fact that one out of four points plots outside the alignment.

The Somme Pluton, 40 km long north south and at least 25 km wide, occupies the southern core of the Kenogamissi granitic complex. It is one of the youngest phases, regionally cross-cutting both the hornblende and biotite tonalites. The Somme Pluton consists of massive to weakly foliated, equigranular, biotite granite to granodiorite and associated pegmatitic and aplitic dykes. Crude igneous layering is locally developed. A distinctive characteristic of the Somme Pluton is the development of large, kilometre-wide areas of coarse-grained pegmatitic granite exhibiting spectacular megascopic graphic intergrowth textures. Along its southern margin the Somme Pluton intrudes the ca. 2682 Ma Neville Pluton creating a three-kilometre wide transition zone characterized by alternating sheeted dykes and large xenoliths of Neville hornblende granodiorite. A massive biotite-granite (sample 41) yields a scatter of 4 discordant zircon analyses. A line through the least discordant point E and the most discordant point P yields an upper intercept age of 2684 ± 4 Ma (Fig. 16), which is interpreted as a maximum age for igneous emplacement and crystallization, consistent with a U-Pb SHRIMP age for the granite of 2676 ± 4 Ma (J.W.F. Ketchum, unpub. SHRIMP U-Pb data).

Two concordant titanite analyses yield two $^{207}Pb/^{206}Pb$ ages of 2615 ± 3 Ma and 2576 ± 2 Ma, while a third is strongly discordant. The discrepancy suggests that these ages reflect mineral growth below the closure temperature of titanite. Three concordant analyses of single monazite grains have $^{207}Pb/^{206}Pb$ ages 2581 ± 4 Ma, 2568 ± 4 Ma, and 2540 ± 4 Ma. Abnormally low and variable Th/U ratios, as compared to most igneous and metamorphic monazite, are indicated by $^{208}Pb/^{206}Pb$ ratios ranging from 0.32 to 0.05. Low Th/U ratios in monazite indicate low temperature growth from hydrothermal solutions (Overstreet, 1967).

DISCUSSION

Age evidence for stratigraphic conformity

U-Pb TIMS ages place stratigraphic controls on at least five volcanic groups in the Swayze belt that can be correlated with major assemblages across the southern Abitibi belt thus supporting a consistently upward younging stratigraphy (Goodwin, 1977). A plot of igneous ages (Fig. 17) shows the change, at the present erosional level, from volcanism and plutonism to dominantly plutonism over time. None of these ages are out of sequence with the upward facing stratigraphy.

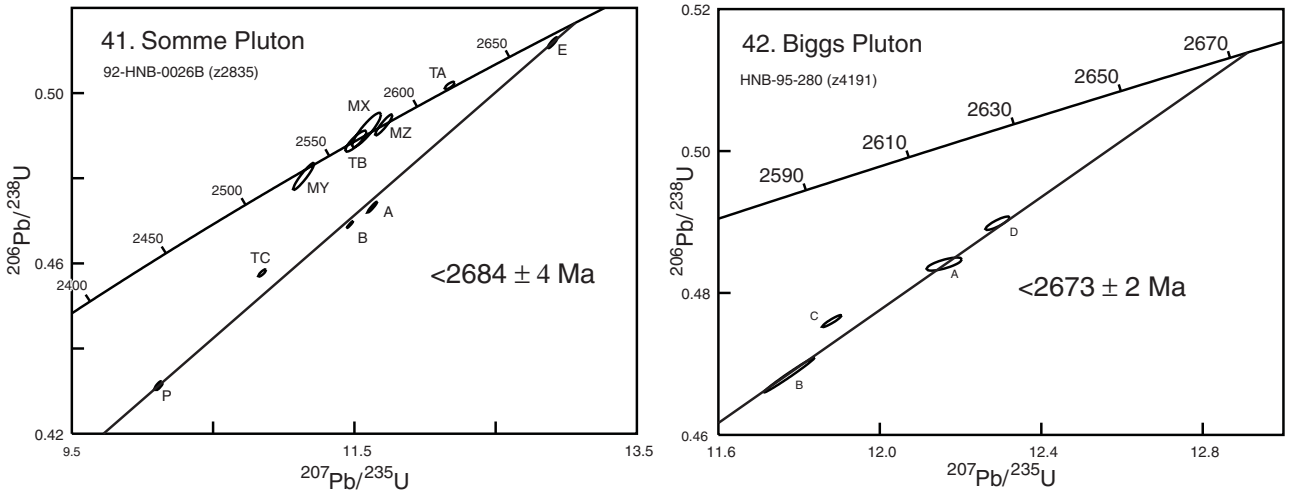

Figure 16. U-Pb concordia diagrams for zircon analyses from post-tectonic plutons: Somme Pluton and Biggs Pluton.

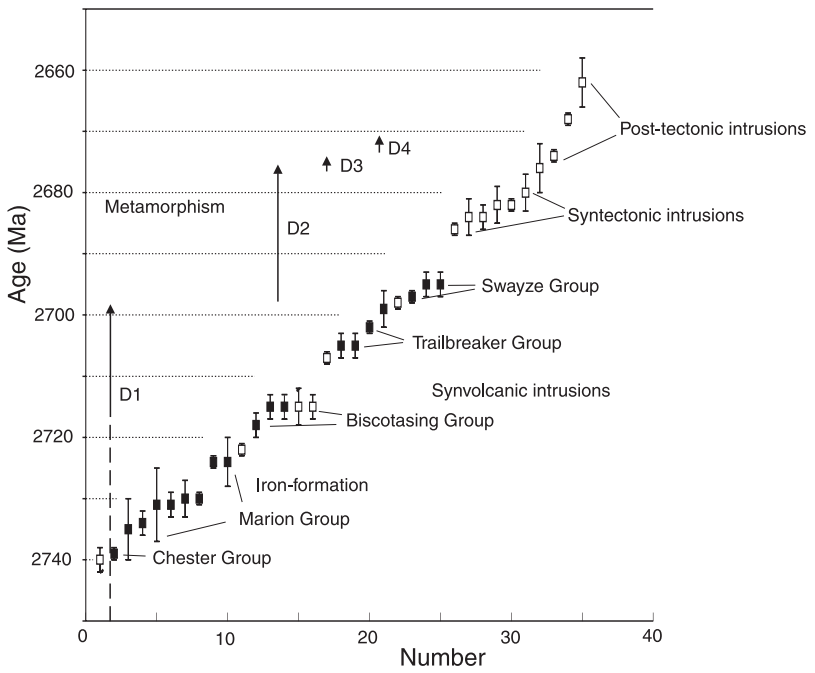

Figure 17. Plot of volcanic (closed rectangles) and plutonic (open rectangles) ages, in order of decreasing age. Estimates of duration of deformation are from Heather (2001, Fig. 2.15).

A number of crosscutting porphyry dykes dated during this study are interpreted to be feeders to overlying volcanic rocks. For example, sample 2 comes from a quartz-phyric felsic rock cutting the ca. 2740 Ma Chester Group in the core of the Woman River anticline, but is interpreted as a synvolcanic feeder to the ca. 2730 Ma Strata Lake Formation of the Marion Group. The Marion Group, in turn, is cut by numerous mafic and ultramafic dykes that are interpreted as feeders to the overlying mafic to ultramafic volcanic rock packages, such as the October Lake Formation (Fig. 3). In the same section the, Marion Group is cut by a quartz-feldspar porphyry that is likely a feeder to the younger, ca. 2705 Ma old, Heenan Formation. Such cases provide convincing evidence against major tectonic transport and allochthonous relationships (cf. Jackson et al., 1994).

Seven U-Pb ages demonstrate a convincing correlation for the occurrence of an extensive 2.73 Ga iron-formation. As these coeval iron-formation bodies can be traced across the Ridout deformation zone, they constitute the basis for a regional Swayze belt/Abitibi belt marker horizon that allows stratigraphic correlation across major deformation zones. They may also be correlative with iron-formation in the Wawa Subprovince. On the east side of the Kenogamissi granitoid complex, felsic volcanic rocks underlying the iron-formation have been dated as 2727 ± 1.5 Ma (Corfu et al., 1989), which makes them time-correlative with the regional, time-stratigraphic iron-formation in the Swayze belt. Similarly, felsic volcanic rocks associated with the uppermost iron-formation in the Shaw Dome, south of Timmins, have been dated as 2724.1 ± 3.7 Ma (Ayer et al., 2005), which is correlative with the 2724 ± 2 Ma upper iron-formation in the Shunsby sector, Swayze belt. In the central Abitibi belt, the 2730 ± 1 Ma (Mortensen, 1993) felsic volcanic rocks of the Hunter Mine Group are capped by oxide iron-formation and base-metal sulphide bodies at the Normetal Mine. In the Joutel area, near the Agnico-Eagle Mine, felsic volcanic rocks with associated sulphide-rich iron-formation were dated at 2730 +5/-2 Ma by Mortensen (1993). Base-metal sulphide and lean iron-formation (cherty exhalite horizons) are associated with circa 2730 to 2725 Ma felsic volcanic rocks at the Selbaie and Matagami camps. In the Chibougamau area, the Lac Sauvage iron-formation caps circa 2730 to 2727 Ma felsic volcanic rocks of the Waconichi Formation (Mortensen, 1993).

Stratigraphic conformity is also supported by detrital zircons from the Denyes Formation of Swayze Group that were derived from the immediately underlying volcanic rocks of the Brett Formation and the Trailbreaker Group. A proximal origin for the Denyes Formation is also consistent with the general absence of rounding of detrital zircons. In contrast, sediments from the Opeepeesway Formation of the Ridout Group were mostly derived from deeper levels in the succession, with ages equivalent to Chester Group. A deeper level origin is consistent with the unconformable relationship of the Ridout Group to underlying volcanic rocks along major east-west fault structures of the Swayze belt.

The 'layer cake' stratigraphy in the Swayze belt, the regional stratigraphic correlations across the Abitibi Subprovince (Davis et al., 2000; Ayer et al., 2002) and the presence of older stratigraphic units in the southern Abitibi are not consistent with Cenozoic-style subduction related tectonic models, as these are fundamentally based on the concept of southward-migrating linear belts, narrow magmatic arcs, and tectonic breaks between distinct terranes. Furthermore, the fact that at approximately 2730 to 2725 Ma ago there were similar environments, depositing felsic volcanic

rocks and iron formation-, across the entire Abitibi suggests a uniform tectonic regime and the possibility of regional correlation. Although the evidence is not conclusive, a plume-related model would be more consistent with 1) the widespread mafic and utramafic rocks, including komatiite, and 2) the regionally correlative stratigraphy with extensive coeval iron-formation bodies. Alternatives should therefore be sought to a Cenozoic subduction model, either in terms of a modified Archean subduction regime, an Archean mantle plume, or a combination of both (cf. Bleeker et al., 1999).

Plutonism and tectonic setting

Plutonism lasted from 2.74 Ga to 2.66 Ga, during the entire period of volcanism and subsequent sedimentation. In both the Kenogamissi Batholith and the Ramsey-Algoma granitoid complexes there is a temporal progression, based on crosscutting relationships and geochronology, from 1) early, more mafic, hornblende-rich diorite through 2) hornblende and biotite tonalite and granodiorite to 3) more felsic, hornblende and biotite-bearing granodiorite and granite. The 2722 ± 2 Ma age for the tonalitic orthogneiss from Gogama (sample 24) is clearly a synvolcanic intrusion, not basement. Syntectonic plutons constrain around 2680 Ma the main, D_2 deformation event, which established the map pattern of the Swayze belt. This was also a period of orogen-wide shortening across the entire Superior Province event that coincided with gold mineralization.

Post-tectonic plutons as young as 2.66 Ga are also found across the Superior Province, mainly within large granitoid complexes. Titanite ages from the Somme Pluton range from 2615 Ma to 2540 Ma and are 50 to 150 Ma younger than the latest plutonism in the Swayze belt. Similar ages were reported by Krogh (1993) from the Kapuskasing zone where U-Pb zircon ages showed that ductile deformation continued at depth till 2585 Ma and where U-Pb titanite ages showed a metamorphic adjustment to have occurred ca. 2500 Ma. Titanite growth in the Somme Pluton is most likely related to late stage fluids resulting from continuing high temperatures and deformation at depth.

Both the plutonic and the volcanic rocks contain evidence of inheritance with ages that do not exceed those obtained from igneous rocks in the Swayze belt. Inherited ages in igneous rocks are in every case found in multigrain fractions of normally ten zircons. Because these are mixed ages, they provide minima for the inherited component and cannot be used to identify the stratigraphic level of the source rock (c.f. Heather, 1998). However, U-Pb SHRIMP spot analyses from two post-tectonic granites also show no inherited ages older than igneous rocks from the Swayze belt (O. van Breemen, unpub. SHRIMP U-Pb data). There is, furthermore, no evidence for an older age contribution amongst detrital zircons from three metasedimentary samples (Fig. 18). So neither the data from xenocrystic zircon in granite, detrital zircon in sediments, nor the 2.72 Ga age for the tonalitic gneiss from Gogama support the existence of pre-volcanic basement; i.e.

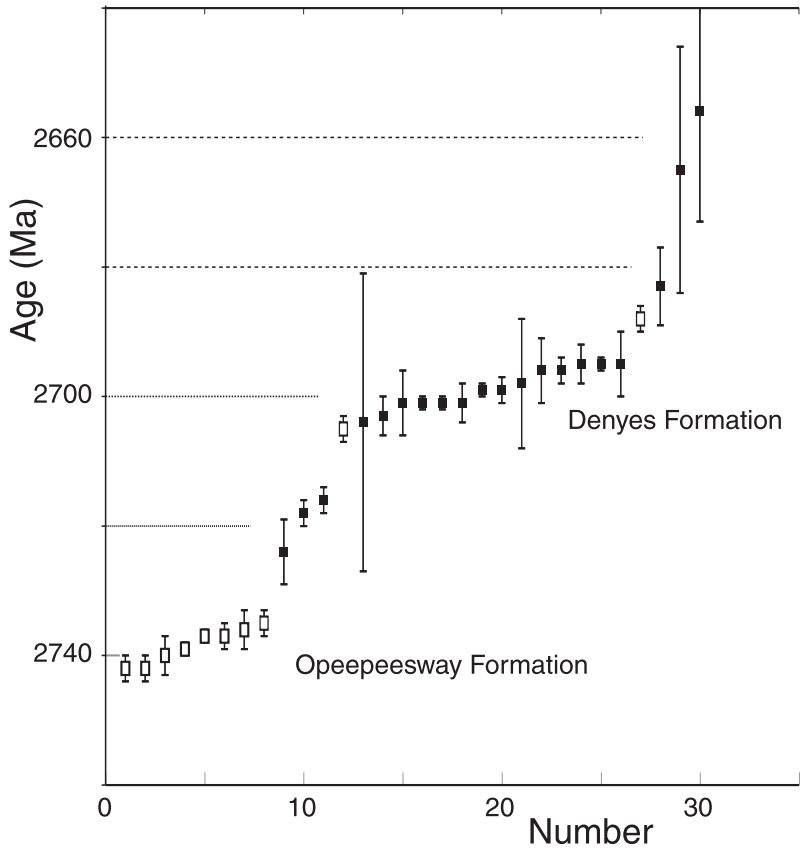

Figure 18. Plot of detrital zircon ages from the Denyes Formation, Swayze Group (closed rectangles) and the Opeepeesway Formation, Ridout Group (open rectangles), showing older detrital ages for younger sediments deposited in a tectonically active setting.

they support a juvenile setting for the development of the Swayze belt. The data presented are limited, however, and for a full discussion about other isotopic evidence and the nature of pre–Abitibi belt crust, the reader is referred to Bleeker (2002).

ACKNOWLEDGMENTS

The authors thank Jack MacRae, Diane Bellerive, and Klaus Santowski for their contributions to the analytical work. Critical reading by Vicki McNicoll is greatly appreciated.

REFERENCES

Ayer, J., Amelin, Y., Corfu, F., Kamo, S., Ketchum, J, Kwok, K., and Trowell, N.
2002: Evolution of the southern Abitibi greenstone belt based on U-Pb geochronology: authochthonous volcanic construction followed by plutonism, regional deformation and sedimentation; Precambrian Research, v. 115, p. 63–95.

Ayer, J.A., Thurston, P.C., Bateman, R., Dubé, B., Gibson, H.L., Hamilton, M.A., Hathway, B., Hocker, S.M., Houlé, M.G., Hudac, G., Ispolatov, V.O., Lafrance, B., Lesher, C.M., MacDonald, P.J., Péloquin, A.S., Piercey, S.J., Reed, L.E., and Thompson, P.H.
2005: Overview of results of the Greenstone Architecture Project: Discover Abitibi Initiative; Ontario Geological Survey, Open File Report 6154, 146 p.

Bleeker, W.
2002: Archaean tectonics: a review, with illustrations from the Slave craton; *in* The Early Earth: Physical, Chemical and Biological Development, (ed.) C.M.R. Fowler, C.J. Ebinger, and C.J. Hawkesworth; Geological Society of London, Special Publication 199, p. 151–181.

Bleeker, W., Parrish, R.R., and Sager-Kinsman, A.
1999: High-Precision U-Pb geochronology of the late Archean Kidd Creek deposit and surrounding Kidd Volcanic Complex; *in* The Giant Kidd Creek Volcanogenic Massive Sulfide Deposit, Western Abitibi Subprovince, Canada, (ed.) M.D. Hannington and C.T. Barrie; Economic Geology Monograph 10, p. 43–70.

Cattell, A., Krogh, T.E., and Arndt, N.T.
1984: Conflicting Sm-Nd whole rock and U-Pb zircon ages for Archean lavas from the Newton Township, Abitibi Belt, Ontario; Earth and Planetary Science Letters, v. 70, p. 280–290.

Corfu, F., Krogh T. E., Kwok, Y.Y., and Jensen, L.S.
1989: U-Pb zircon geochronology in the southwestern Abitibi greenstone belt, Superior Province; Canadian Journal of Earth Sciences, v. 26, p. 1747–1763.

Davis, W.J., Lacroix, S., Gariépy, C., and Machado, N.
2000: Geochronology and radiogenic isotope geochemistry of plutonic rocks from the central Abitibi subprovince: significance to the internal subdivision and plutono-tectonic evolution of the Abitibi belt; Canadian Journal of Earth Sciences, v. 37, p. 117–133.

Frarey, M.J. and Krogh, T.E.
1986: U-Pb zircon ages of late internal plutons of the Abitibi and eastern Wawa subprovinces, Ontario and Quebec; *in* Current Research, Part A, Geological Survey of Canada Paper 86-1A, p. 43–48.

Goodwin, A.M.
1977: Archean basin-craton complexes and the growth of Precambrian shields; Canadian Journal of Earth Sciences, v. 14, p. 2737–2759.

Heather, K.B.
1998: New insights on the stratigraphy and structural geology of the Southwestern Abitibi greenstone belt: implications for the tectonic evolution and setting of mineral deposits in the Superior Province; *in* The First Age of Giant Ore Formation: Stratigraphy, Tectonics and Mineralization in the Late Archean and Early Proterozoic, Toronto, Prospectors and Developers Association of Canada Annual Convention, p. 63–101.
2001: The geological evolution of the Archean Swayze Greenstone Belt, Superior Province, Canada; Ph.D thesis, Keele University, Keele, England, 370 p.

Heather, K.B. and Shore, G.T.
1999: Geology, Swayze greenstone belt; Geological Survey of Canada, Open File 3384a, scale 1:50 000.

Heather, K.B. and van Breemen, O.
1994: An interim report on geological, structural, and geochronological investigations of granitoid rocks in the vicinity of the Swayze greenstone belt, southern Superior Province, Ontario; *in* Current Research 1994-C, Geological Survey of Canada, p. 259–268.

Heather, K.B., Shore, G.T. and van Breemen, O.
1995: The convoluted "layer-cake", an old recipe with new ingredients for the Swayze greenstone belt, southern Superior Province, Ontario; *in* Current Research 1995-C, Geological Survey of Canada, p. 1–10.

Jackson, S.L. and Fyon, A.J.
1991: The Western Abitibi Subprovince in Ontario; *in* Geology of Ontario, Ontario Geological Survey, Special Volume 4, p. 405–482.

Jackson, S.L., Fyon, A.J., and Corfu, F.
1994: Review of Archean supracrustal assemblages of the southern Abitibi greenstone belt in Ontario, Canada: products of micro-plate interactions within a large-scale plate-tectonic setting; Precambrian Research, v. 65, p. 183–205.

Jolly, W.T.
1978: Metamorphic history of the Archean Abitibi belt; *in* Metamorphism in the Canadian Shield, (ed.) J.A. Fraser and W.W. Heywood; Gelogical Survey of Canada Paper 78-10, p. 63–78.

Krogh, T.E.
1973: A low contamination method for hydrothermal decomposition of zircon and extraction of U and Pb for isotopic age determinations; Geochimica et Cosmochimica Acta, v. 377, p. 485–494.

Krogh, T.E.
1982: Improved accuracy of U–Pb ages by the creation of more concordant systems using an air abrasion technique; Geochimica et Cosmochimica Acta, v. 46, p. 637–649.

Krogh, T.E. (cont.)
1993: High precision U-Pb ages for granulite metamorphism and deformation in the Archean Kapuskasing structural zone, Ontario: implications for structure and development of the lower crust; Earth and Planetary Science Letters, v. 119, p. 1–18.

Mortensen, J. K.
1993: U-Pb geochronology of the eastern Abitibi Subprovince. Part 2: Noranda - Kirkland Lake area; Canadian Journal of Earth Sciences, v. 30, p. 29–41.

Overstreet, W.C.
1967: The geologic occurrence of monazite; a review of the distribution of monazite and of the geologic controls affecting the amount of thorium in monazite; United States Geological Survey, Professional Paper 530, 327 p.

Parrish, R.R., Roddick, J.C., Loveridge, W.D., and Sullivan, R.W.
1987 : Uranium-lead analytical techniques at the Geochronology Laboratory, Geological Survey of Canada; *in* Radiogenic Age and Isotopic Studies: Report 1, Geological Survey of Canada, Paper 87-2, p. 3–7.

Percival, J.A.
1986: A possible exposed Conrad discontinuity in the Kapuskasing uplift, Ontario; *in* The Continental Crust, (ed.) M. Barazangi and L. D. Brown; American Geophysical Union, Geodynamics Series, v. 14, p. 135–141.

Percival, J.A. and Card, K.D.
1983: Archean crust as revealed in the Kapuskasing uplift; Geology, v. 11, p. 323–326.

Percival, J.A. and Krogh, T.E.
1983: U-Pb zircon geochronology of the Kapuskasing structural zone and vicinity in the Chapleau-Foleyet area, Ontario; Canadian Journal of Earth Sciences, v. 20, p. 830–843.

Roddick, J.C.
1987: Generalized numerical error analysis with application to geochronology and thermodynamics; Geochemica et Cosmochemica Acta, v. 51, p. 359–362.

York, D.
1969: Least squares fitting of a straight line with correlated errors; Earth and Planetary Science Letters, v. 5, p. 320–324.

Geological Survey of Canada Project TGI III

APPENDIX I

Analytical techniques

Isotope dilution and thermal ionisation techniques for measuring U–Pb isotopes in zircon at the Geological Survey of Canada are summarized by Parrish et al. (1987), and are based on Krogh (1973). Prior to analysis, all zircon fractions were strongly abraded until the crystals assumed a well-rounded shape (Krogh, 1982). Abrasion was used to minimize the effects of peripheral lead loss and/or to remove rims inferred to have grown during later metamorphism. Mass spectrometry, data reduction, and method of propagation of analytical uncertainties of the relevant components in the calculation of isotopic ratios and ages followed the numerical procedure of Roddick et al. (1987). A modified form of York's (1969) method for linear regression analysis was used (*see* Parrish et al., 1987). Ages are calculated either as weighted average $^{207}Pb/^{206}Pb$ ages or as upper concordia intercept ages (Table 2, 4). Mean squares of weighted deviates (MSWD) provide a measure of the scatter of data points, where values in excess of 2.5 indicate a significant amount of scatter beyond what could be expected from analytical uncertainty alone. U-Pb data is plotted on concordia diagrams in Figures 5 to 9. All TIMS age uncertainties are given at the 95% confidence level.